

**Determination of the steady-state  
performance of a 28 [cm<sup>3</sup>] Innas  
Variable Floating Cup Pump  
(FCV28)**

Dr.ir. W. Post

CST 2010.011

CST Report

Eindhoven University of Technology  
Department of Mechanical Engineering  
Control Systems Technology Group

Eindhoven, March 2010

# Contents

<b>1</b>	<b>Scope of the steady-state performance of a variable pump</b>	<b>3</b>
<b>2</b>	<b>Test pump and operating conditions</b>	<b>4</b>
	General data of the test pumps	4
	Range of requested steady-state operating points	4
	Brief description of the type of pump	4
<b>3</b>	<b>Definitions</b>	<b>6</b>
<b>4</b>	<b>Calculation of derived capacity</b>	<b>8</b>
<b>5</b>	<b>Test circuit</b>	<b>9</b>
	Hydraulic system	9
	Measurement devices	10
<b>6</b>	<b>Class of measurement accuracy</b>	<b>12</b>
<b>7</b>	<b>Test procedures</b>	<b>14</b>
	Test fluid	14
	Temperatures	15
	Steady-state conditions	15
	Test measurements	15
<b>8</b>	<b>Test results</b>	<b>16</b>
8.1	Measurement of the 100% swashed pump (swash-angle: 8 degrees)	17
8.2	Measurement of the 75% swashed pump (swash-angle: 6 degrees)	22
8.3	Measurement of the 50% swashed pump (swash-angle: 4 degrees)	27
8.4	Measurement of the 25% swashed pump (swash-angle: 2 degrees)	32
8.5	Combination of errors (ISO 4409)	37
8.6	Conclusions of measurements	39
	<b>References</b>	<b>40</b>
<b>A</b>	<b>Appendix</b>	<b>41</b>
A.1	Classes of measurement accuracy ISO 4409 and ISO 8426	41
A.2	Errors and classes of measurement accuracy	43

# 1 Scope of the steady-state performance of a variable pump

Determination of the performance of variable positive displacement pump by means of measurements under steady-state conditions. The following properties were determined:

- The total efficiency over a range of operating points. This determination closely follows the ISO 4409 standard (Hydraulic fluid power - Positive Displacement pumps, motors and integral transmissions - Determination of steady-state performance). The measurement accuracy complies to this standards requirements for a class A rating. The selected operating points, however, were set more loosely than the ISO 4409 standard requires for a class A rating. The background to this choice is discussed in section 6.
- The derived capacity according to the guidelines of standard ISO 8426 (Hydraulic fluid power - Positive Displacement pumps and motors - Determination of derived capacity)
- The hydro-mechanical and volumetric efficiency with aid of the derived capacity over a range of operating points.

## 2 Test pump and operating conditions

### General data of the test pumps

Manufacturer:	INNAS BV, Breda, the Netherlands
Type:	Variable Floating Cup axial piston pump (FCV28)
Maximum displacement (geometric):	28.11 [cm <sup>3</sup> /rev]

### Range of requested steady-state operating points:

• Pressure:	50 - 100 - 150 - 200 - 250 - 300 - 350 [Bar]
• Rotational speed:	500 - 1000 - 1500 - 2000 - 2500 - 3000 [rpm]
• Swash angles:	8 - 6 - 4 - 2 [degrees]
equivalent relative displacement	100 - 75 - 50 - 25 [%]
• Oil temperature:	40 [°C]
• ISO viscosity grade:	46
• Boost pressure:	3 [Bar]

Determination of the total efficiency, determination of the derived capacity and determination of the hydro-mechanical and volumetric efficiency under these operating conditions.

The set up of the test circuit and general considerations for testing etc. according to the standards of ISO 4409 and ISO 8426 are in common. Both standards can be combined conveniently for the determination of the complete performance of the pump. Only the calculation of derived capacity according to the standard of ISO 8426 is replaced by a different method. (See section 4).

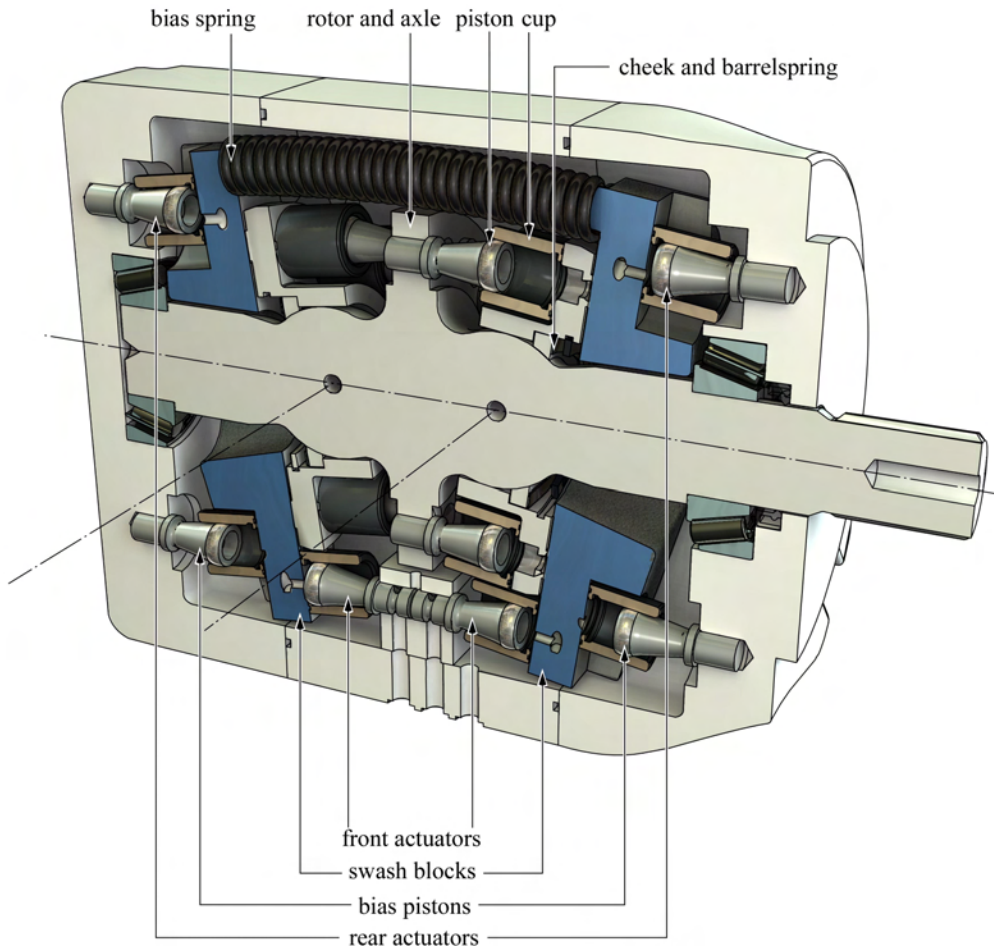
### Brief description of the type of pump

Figure 1 shows the construction of the 28 [cm<sup>3</sup>] Floating Cup Variable (FCV) axial piston pump. The rotary group of this unit is identical to that of a constant displacement FC pump. The displacement volumes in this rotary group are 24 separate cylinders, the cups, which float under a light axial balance force on two barrel plates. In each cup, a piston with a spherical piston head moves between the top- and bottom dead center. No piston rings are used. As the sealing line between the piston head and the wall of the cup, is always perpendicular to its central axis, the internal pressures acting in radial direction on the cylinder walls are totally balanced. Because of this, and because of the absence of piston rings, there are no pressure dependent contact forces between cup and piston. In conventional axial piston units, pressure induced side forces between the pistons and the side walls are an important source of hydromechanical losses. This also explains the rather poor starting and low speed capabilities of conventional units.

The pistons in the FC design are rigidly mounted in two groups of twelve, one on each side of a rotor. The rotor is rigidly mounted on the axle. The oil flow in and out of the unit is split up over two port plates, one on each side of the unit. Always, the same number of pistons on each side of the rotor is connected to the high pressure port. This results in a rotor that is totally balanced in axial direction. Consequently, the loads on the axle bearings are light and relatively small bearings can be chosen.

The barrel rotation is synchronized to the axle rotation by means of synchronization pins, localized in the spherical joints between axle and barrels. A sprung ring, (the “cheek”) ensures that there is always a minimum force pressing the barrel on the port plate. Under pressure, the resulting force between barrels and port plates is the sum of this spring force and the carefully selected hydraulic barrel balance. Setting the barrel balance is subject to optimization: setting it too light will result in low loss torques between barrels and port plates but may lead to high leakage in this interface, setting it too high would result in low leakage but at the cost of high loss torques in this interface. In the FC design, this is the interface which is responsible for the largest part of the loss torques, and therefore it is very important that the barrel balance is carefully set.

In the FCV, the port plates do not lie directly on faces in the units case but on top of two swash blocks. The swash blocks determine the displacement of the machine by tilting the barrel plates



**Figure 1:** Construction of the 28 cm<sup>3</sup> variable displacement open circuit FC pump (FCV28).

with respect to the rotor. Each swash block can be rotated around its respective swash axis by a set of two actuators that work against the forces of a bias spring and a bias piston that is always connected to the unit's high pressure. The actuators and compensators are piston and cup combinations of the same size as those used in the rotary group. In this way the production costs for the swashing system are minimized.

During the measurements series described in this report, the swash-blocks were fixed in the required position by two sets of eccentric discs, one set for each swash-block. The bias springs, the bias pistons and the actuator pistons were not present. On one hand, the absence of the forces generated by these pistons, means that the swash blocks are not ideally loaded and will bend more, which will lead to larger gaps and more leakage. On the other hand, the leakage which normally comes from the six piston-cup sets of the swashing system, is absent. The combined effect on the measured efficiency is considered to be small.

### 3 Definitions

Definitions are mostly according paragraph 3 of ISO 4409 (respectively, paragraph 3 of ISO 8426), with paragraph number in parenthesis. Otherwise definitions are from the common theory regarding positive displacement pumps, see the text books concerning Fluid Power Transmissions, for example Ivantysyn [1].

- Volume flow rate  $q_V$  [m<sup>3</sup>/s] : The measured flow volume per unit of time. (3.1.1)
  - drainage flow rate  $q_{Vd}$  [m<sup>3</sup>/s] : the volume flow rate of flow from the casing. (3.1.2)
  - effective outlet flow of a pump  $q_{V2,e}^P$  [m<sup>3</sup>/s] : the actual flow rate measured at the pump outlet at the temperature  $\theta_{2,e}$  and pressure  $p_{2,e}$  at the outlet of the pump. (3.1.3)
- Rotational frequency (shaft speed)  $n$  [1/s] : The number of revolutions of the shaft per unit of time. (3.2)
- Torque  $T$  [Nm] : The measured value of the torque in the shaft of the test component. (3.3)
- Pressure: (3.4.1)
  - effective pressure  $p_e$  [Pa] or [N/m<sup>2</sup>] : The fluid pressure, relative to atmospheric pressure.
  - drainage pressure  $p_d$  [Pa] or [N/m<sup>2</sup>] : The fluid pressure, relative to atmospheric pressure, measured at the outlet of a drainage connection on a component casing.
- Power:
  - Mechanical power  $P_m$  [W] : the product of the torque and rotational frequency measured at the shaft of a pump. (3.5.1)

$$P_m = 2\pi \cdot nT$$

- Hydraulic power  $P_h$  [W] : the product of the flow rate and the pressure at any point. (3.5.2)

$$P_h = q_v \cdot p$$

- Effective outlet hydraulic power of a pump  $P_{2,h}^P$  [W] : the total outlet power of pump. (3.5.3)
- Efficiency
  - pump overall efficiency  $\eta_t^P$  [-] : The ratio of the power transferred to the liquid, at its passage through the pump, to the mechanical input power. (3.6.1)

$$\eta_t^P = \frac{(q_{V2,e} \cdot p_{2,e}) - (q_{V1,e} \cdot p_{1,e})}{2\pi \cdot nT} \quad (1)$$

NOTE: Index 1 refers to the inlet of the pump.

- pump volumetric efficiency  $\eta_v^P$  [-] : The ratio of the effective outlet flow rate  $q_{V2,e}$  of the pump, to the theoretical outlet flow rate  $q_{Vi}$  of the pump:

$$\eta_v^P = q_{V2,e} / q_{Vi} \quad (2)$$

Where:

$$q_{Vi} = n \cdot V_i^P \quad (3)$$

and  $V_i^P$  is the derived capacity of the pump.

- pump hydro-mechanical efficiency  $\eta_{hm}^P$  [-] : the ratio of the theoretical torque  $T_i$  in the shaft of the pump, to the measured value of the torque  $T$  in the shaft of the pump.

$$\eta_{hm}^P = T_i / T \quad (4)$$

Where:

$$T_i = (p_{2,e} - p_{1,e}) \cdot V_i^P / 2\pi \quad (5)$$

and  $V_i^P$  is the derived capacity of the pump.

- Derived capacity  $V_i^P$  [m<sup>3</sup>/rev] : the volume of the fluid displaced by the pump per shaft revolution, calculated from measurements at different speeds under test conditions, see section 4.

## 4 Calculation of derived capacity

The standard of ISO 8426 deals with the determination of derived capacity of a pump (or motor). For the definition of derived capacity see section 3. The value found for the derived capacity usually differs from the geometric displacement. Since this capacity is calculated from measurements on a unit under operating conditions all events contributing to the effective volume flow are included. Depending on type of the positive displacement unit the derived capacity deviates about 2 to 3% from the geometric displacement according to Schlösser [2].

The standard of ISO 8426 states that the test should be carried out at an outlet pressure of approximately 5% of the maximum continues rated pressure of the unit. In this case these measurements require a set point of about 17.5 [Bar] for the outlet pressure of the pump. The calculation of the derived capacity has to be made from that condition. Unfortunately, this requirement usually implies an extra set of measurements, because the stated pressure is (considerably) lower than the lowest pressure setting in the set of operating points. Furthermore this method does not eliminate the effects of leakage (or slip loss), nor is assured that the stated pressure results in a proper stable operation of the pump. Reason to use a calculation method based on the complete set of operating points and eliminating the effect of leakage due to a pressure difference unequal to zero.

A number of institutes (in Europe) prefer the calculation method according to Toet [3]. This method is also customary in the determination of the steady-state performance of positive displacement units in our laboratory.

The derived capacity according to Toet [3] is calculated from the complete field of operating points and is defined as:

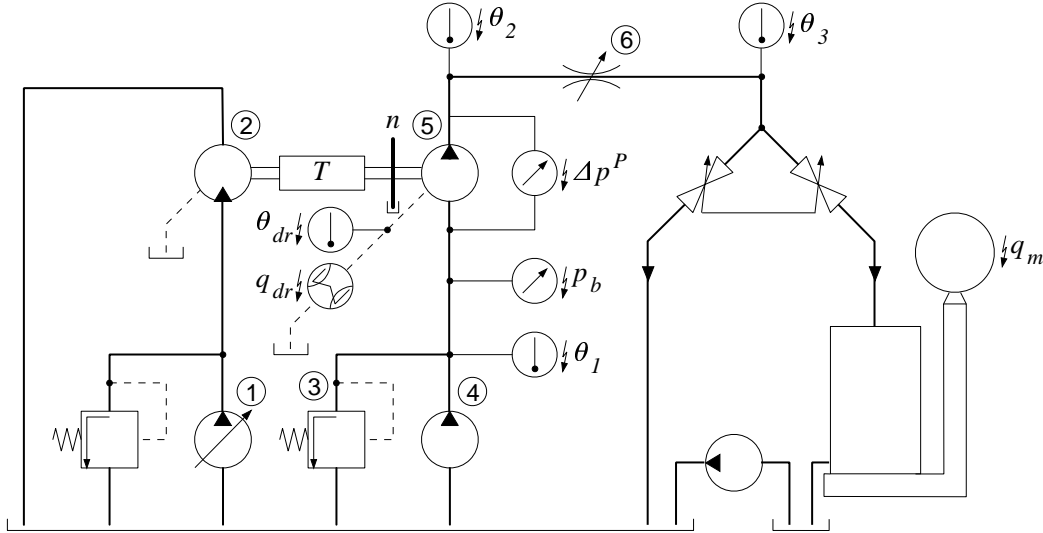
$$V_i^P = \left( \frac{\partial q_{V2,e}}{\partial n} \right)_{(p_{2,e}-p_{1,e}=0, \theta_1)} \quad (6)$$

The calculation of the derived capacity is performed in two steps. The values of the effective flow gradient at each set point for the pressure difference are calculated first. The underlying basic assumption is, that for every set point for the pressure difference, there is a linear relationship between effective flow and speed, which yields the effective flow gradient. This step is followed by an extrapolation of the fitted line through the flow gradient values, to the point where the pressure difference across the pump equals zero. Note that the derived capacity according to Toet depends on the temperature of the fluid (inlet condition of the unit).



## 5 Test circuit

For measurements a test circuit according to the basic open test circuit with pump outlet flow measurement in alternative position (as stated in ISO 4409/8426) is used. Figure 2 displays the actual setup of the test circuit .



### Hydraulic circuit

- |                                    |                                     |
|------------------------------------|-------------------------------------|
| 1. Pump B & C (Hyd. Power Unit)    | 4. Make up pump D (Hyd. Power Unit) |
| 2. Motor Volvo F11-58              | 5. Pump under test                  |
| 3. Pressure relief valve (3 [bar]) | 6. Pressure-control valve           |
- Hyd. Power Unit: Temperature control, filtering and conditioning of fluid

### Measurement devices

$T$	Torque transducer	$\theta_2$	Temperature transducer outlet pump
$n$	Rotational speed transducer	$\theta_3$	Temperature transducer inlet bascule
$\theta_1$	Temperature transducer inlet pump	$q_m$	Weight sensor (Mass flow) bascule
$p_b$	Pressure transducer inlet pump	$\theta_{dr}$	Temperature transducer drain pump
$\Delta p^P$	Differential pressure transducer	$q_{dr}$	Flow transducer drain pump

**Figure 2:** *Hydraulic Setup*

### Hydraulic system

Part of the installation consists of a central hydraulic power unit, which includes the make-up of the fluid (filtering and cooling or heating of the fluid, elimination of entrapped air etc.) The test pump (5) requires a pressurized inlet condition. A boost pump (4) with sufficient capacity and an additional pressure relief valve (3) is used for the make-up flow of the test pump. The test pump (5) is coupled to a fixed displacement hydro motor by means of the torque shaft (T) and is loaded by means of a pressure control valve (6). The latter consists actually of a number of valves, which are operated manually, for the purpose of fine tuning of the pressure setting. The setting of the rotational speed (n) is realized by means of variable displacement pumps (1) in the central hydraulic power unit.

**Note:**

For the hydraulic motor (2) a Volvo F11-58 is used for driving the pump under test (5) at swash angles of 8 and 6 degree and a Volvo F11-39 at swash angles of 4 and 2 degree.

**Measurement devices**

- Torque: HBM (Hottinger Baldwin Messtechnik) T2/200 Nm torque measuring shaft + HBM MGC strain-gage bridge amplifier;
- Rotational speed: Optical/disk 100 pulses/rev. (GTD TU/e) + Phoenix Contact MCR F/V converter;
- Temperature: Heraeus PT 100 sensor 4-20mA output + Ti66/A I/V conditioner (GTD TU/e);
- Inlet pressure pump: Druck PTX 1400 pressure transmitter 4-20 mA output;
- Differential pressure pump: Paine 5000 PSID Bi-directional differential pressure transducer + HBM MVD2555 strain-gage bridge amplifier;
- Bascule (weight): Raute BA3 load cells (inclusive pendulum support mounting RGP10) + Weightec 341AD4, analog/digital load cell amplifier with built-in junction box.
- Drainage flow: VSE VS0.2 flow sensor + Phoenix Contact MCR-f-UI-DC F/V converter

Unlike the standard of ISO 4409, ISO 8426 specifies an integrating flow meter for the measurement of the effective outlet flow rate of a pump. It is customary to use integrating (or averaging) methods for all signals in the set-up of steady-state measurements in our laboratory. So the requirement of ISO 8426 is fulfilled.

It is also customary in our laboratory to use a mass flow rate measurement instead of a volume flow rate measurement. In order to calculate the volume flow rate  $q_{Ve,2}$  from the measured mass flow  $q_m$  the fluid properties (in particular the state of the fluid  $\rho(p, \theta)$ ) should be available. The fluid properties of the test fluid can be determined by any model of the state. In our laboratory it is customary to use the model of state  $\rho(p, \theta)$  according to Witt [5]. The measurement of the mass flow is actually based on an integrating device, in this case an weighting device. Using the mass flow  $q_m$  circumvents the problems associated with the compressibility of the fluid or uncertainties of this quantity. The volume flow rate can be calculated from the mass flow rate, given that the pressure and temperature are known at the point of interest in the circuit. Apart from leakage, the mass flow rate is a constant quantity. Note that the standard of ISO 4409 proposes a first order approximation for effect of compressibility (based on the assumed constant isothermal secant bulk modulus) in case of a measurement downstream of the pump.

The measurement set up consists of measuring instruments, including the necessary conditioning and conversion of the signals, and a data acquisition board (National Instruments 6034E Multifunction DAQ) mounted in a PC. All measured signals are converted to voltages prior to be directed to the data acquisition board. The Multifunction DAQ board operates under software control build with LabView (National Instruments). This software control, in the form of a graphical user interface (GUI), monitors all measurement signal, controls a number of devices of the hydraulic system and controls the data logging.

During the time interval of the weighting process the signals of all measuring instruments are recorded for later analysis. The data of all measurement instruments were recorded concurrently with a sample rate of 5000 [Hz] over a time interval of at least 20 seconds. At low speeds and small swash-angles, the time interval was longer (up to 60 seconds), in order to ensure that enough oil mass was measured in the bascule.

The voltage signals of all measurement instruments are recorded on file by means of Direct Memory Access (DMA). Post processing of the recorded data includes averaging, trend analysis and

conversion to physical quantities. Each signal is examined visually before these post processing operations are performed. During this visual inspection the measurement is accepted, a long enough stationary part is cut out or – in the unlikely case that that should not be present – the measurement is discarded. Calculations (total efficiency, derived capacity and part efficiencies) are based on the mean or averaged physical values of the resulting signals.

## 6 Class of measurement accuracy

In the standard of ISO 4409 and ISO 8426 several demands on accuracy are stated. Each demand distinguishes between three classes, from highest to lowest: classes A, B and C. Note that class C is intended for the common case of measurements, while classes A and B are intended for special cases where there is a need to have the performance more precisely defined. Common demands of both standards concern:

- the permissible variation in indicated fluid temperature (demand 1), see appendix A.1 table 1;
- the limits of permissible variation of mean indicated values of selected (or controlled) parameters (demand 2), see appendix A.1 table 2;
- the permissible systematic errors of measuring instruments as determined during calibration (demand 3), see appendix A.1 table 3.

The standard of ISO 8426 also states a demand on the number of pump and motor test speeds (demand 4), see appendix A.1 table 4. While both standards are combined in this test, demand (4) already bounds the actual class of accuracy for this particular test to be of class B at best. From the complete set of measurements it may be concluded that the controlled (or selected) parameters in this test are:

- the fluid inlet temperature of the pump (demand 1): these lie within the variation of temperature of class A for all measurements of each of the pumps.
- the rotational speed of the pump (demand 2)
- the outlet pressure of the pump (demand 2)

For these measurements, it was not attempted to achieve a class A accuracy with respect to demand 2. The requested speed and output pressure points given in section 2, were taken as target and approached as close as possible but in general not within the limits required for a class A accuracy rating. The reasons for this deviation from the class A requirement are:

- In this test-bed setup, setting the desired operating points within the precision required by class A, would be rather time-consuming, as it involves repeated iterations between the setting of the pressure control valve (item 6 in figure 2) and of the variable displacement pumps in the central hydraulic power unit (item 1 in figure 2).
- The background to the demands of these ISO standards regarding the accuracy which of setting the operating points, seems to relate to the presentation of the results. Graphs of the pump performance against the effective output pressure are defined as well as against the rotational frequency. In either case the graphs have to be given for several constant values of the other controlled parameter, for which obvious requirements are set regarding the accuracy of the set point.
- When different performance properties are presented as surface plots against the effective outlet pressure and the rotational frequency, very smooth surfaces will result, which can be described quite well with 42 operation points measured, as long as these operating points define a reasonably well spread grid.

The approach adopted in this test was accordingly:

- Measure the unit under test at operating points which are fairly close to the requested grid,
- Calculate the required performance properties in the points measured
- Fit surface plots to these calculated properties.

The fitted surfaces are presented in the subsections presenting the results for each measured swash angle. Characteristics as a function of effective outlet pressure and of rotational frequency have also been produced by interpolation in the fitted surfaces in order to present the results conform the ISO standards too. The quality of the fit and the interpolation is quite accurate as can be noticed by comparing the values in the tables presenting the actually measured points to the fitted surfaces, .

It should be noted that an important factor to deviate from the standards was the broader context in which this test-bed is used: a research project concerning the identification and minimization of the losses in the interfaces between the barrels and the port plates in Floating Cup units. During the cause of this project, this measurement and post processing protocol has evolved as the best protocol to ensure fast and accurate quantification of the losses in these interfaces, when a large number of prototype variants have to be evaluated.

For the operating points realized this way – which lie near to the target points – the efficiencies are calculated in the way ISO 4409 defines. The calculation results for these points, are precise in accordance with the accuracy of the instrumentation. For this accuracy, the ISO standards also define classes. The systematic errors in the used instrumentation, for the range of operating points of interest (see section 2), are all within the limits of class A of permissible systematic errors (see appendix A2).

## 7 Test procedures

### Test fluid

The fluid used for these tests is the standard hydraulic oil applied in the central hydraulic power supply in our laboratory: Mobil DTE 25.

Summary from the data sheet of: 'Mobil DTE 20 Series Hydraulic Oils':

- Spec. Gravity (15.6 °C): 0.876 [kg/L]
- Viscosity @ 40 °C: 44.2 [cSt]
- Viscosity @ 100 °C: 6.65 [cSt]
- ISO Viscosity Index: 46

The actual value of the density  $\rho(p, \theta)$  of this fluid is calculated from the state model according to Witt [5]. Witt state model for the density contains 7 parameters, which ideally have to be fit for the fluid used. This is a tedious task, as it would involve density measurements at a large number of pressure and temperature set-points. Especially density measurements under pressure, are not easy. As Witt has demonstrated in [6], for mineral hydraulic oils, the concept of a 'calculation fluid' can be used. Thus 5 of the 7 parameters of the state model can be set equal to those determined by Witt for the 'calculation fluid'. The two remaining parameters have to be fit to the actual mineral oil used. These two parameters are the density at ambient pressure and a temperature of 0°C and the gradient of the density-temperature relationship at ambient pressure. The latter two parameters were determined for a sample of the oil from the test bed reservoir, using a pycnometer.

Figure 3 presents the density of the fluid, calculated using the resulting Witt state model, for the demanded test conditions of section 2.

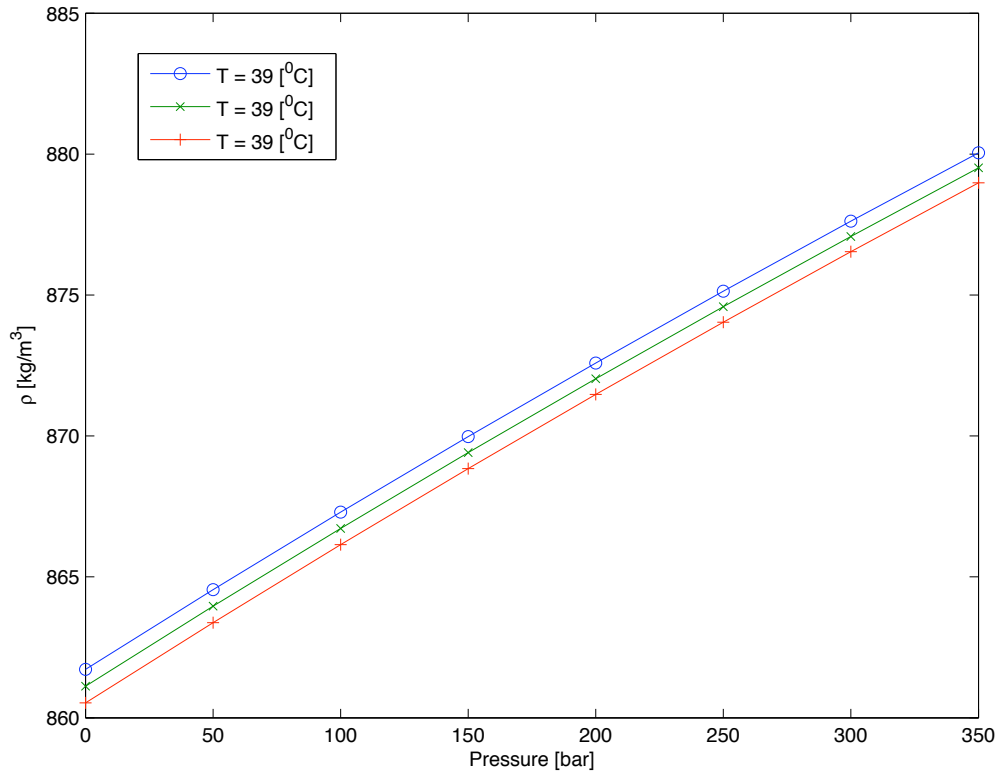


**Figure 3:** Density of the Mobil DTE25 oil used in the testbed

## Temperatures

The temperature at the inlet of the test pump is the controlled temperature. All other measured temperatures are resulting quantities. For the demands regarding the controlled temperature see section 2 and 6, respectively appendix A.1 and A.2.

## Steady-state conditions

When steady-state test conditions are reached for a specific test condition, only one set of individual quantities has to be taken over concurrent common time periods. Each reading has to be recorded as the mean value of each quantity being measured.

In practice it is hardly possible to perform a static, i.e. time invariant measurement on a positive displacement unit (pump or motor) under operating conditions. So the measurements have to be accomplished under quasi stationary conditions. Reason to record the time varying instrument readings and determine the mean values from these records, in our set up. These records also enable to check if the steady-state conditions are actually met. As stated before every recorded signal was visually checked to ensure stationary conditions. If necessary a stationary part was isolated from the measurement. In these four measurement sets, there was never a reason to discard a measurement point completely.

In principle, the values of the controlled parameters should be within the limits given in the classes of measurement accuracy. Here we have deviated from the test procedure, as has been explained in the previous section.

## Test measurements

The controlled quantities in this particular test are the rotational speed  $n$  and the outlet pressure  $p_{2,e}$  of the test pump. The inlet pressure  $p_{1,e}$  and the inlet temperature  $\theta_{1,e}$  of the test pump should be kept constant during each test within the limits of the class of accuracy. All quantities of each set of measurements have to be measured under steady-state conditions. The sets of measurements correspond to the demanded range of rotational speed and of pump outlet pressure, see also section 2 and 5. The range of these sets are selected so as to give a representative indication of the performance of the test pump.

Measurements of the delivered volume flow  $q_{V2,e}$  and torque  $T$  of the test pump are used to determine the total efficiency and the derived capacity. The volume flow  $q_{V1,e}$ , which is also necessary for the calculation of the efficiency, was calculated by adding the drainage mass flow (calculated from the drainage volume flow  $q_{Vd}$  at the drainage flow temperature  $\theta_d$  using the state model of Witt) to the delivered mass flow to determine the inlet mass flow (conservation of mass). This mass flow was converted to the inlet volume flow, using the Witt model and the measured inlet states.

With use of the derived capacity the volumetric and hydro-mechanical efficiencies are determined, see section 2.

## 8 Test results

The results of each of the four swash angles of the test are presented in the following subsections (8.1 to 8.4) . Results are presented in numerical and in graphical form. In graphical form, first the results for the determination of the derived capacity according to the Toet method is presented. Numerical results, including the results of calculations of total- and part efficiencies are presented next. Calculations for each of the quantities presented are according the definitions and formulae of section 3. Finally the graphical results for the total-, the volumetric- and the hydro-mechanical efficiency are presented for each target pressure, as a function of the rotational speed, in the fashion of the standards (ISO 4409 and 8426).

Subsection 8.5 deals with the combination of systematic errors in the calculation of total efficiency of the pumps. And finally in subsection 8.6 some conclusions are drawn from the results of the measurements.



## 8.1 Measurement of the 100% swashed pump (swash-angle: 8 degrees)

Date: 29-Jan-2010

### Properties of Test fluid:

Test fluid:	Mobil	DTE 25
Temperature at inlet:	40.0	[°C] ( $\pm 1.0$ [°C] for all operating points)
Kinematic viscosity:	45.9	[cSt] (or [mm <sup>2</sup> /s])
Density:	861.3	[kg/m <sup>3</sup> ] @ atmospheric conditions and inlet temperature
Inlet pressure:	3.0	[Bar] ( $\pm 2.4$ [%] for all operating points)

### Derived capacity:

Nominal:	28.11	[cm <sup>3</sup> ]
Toet:	27.43	[cm <sup>3</sup> ]

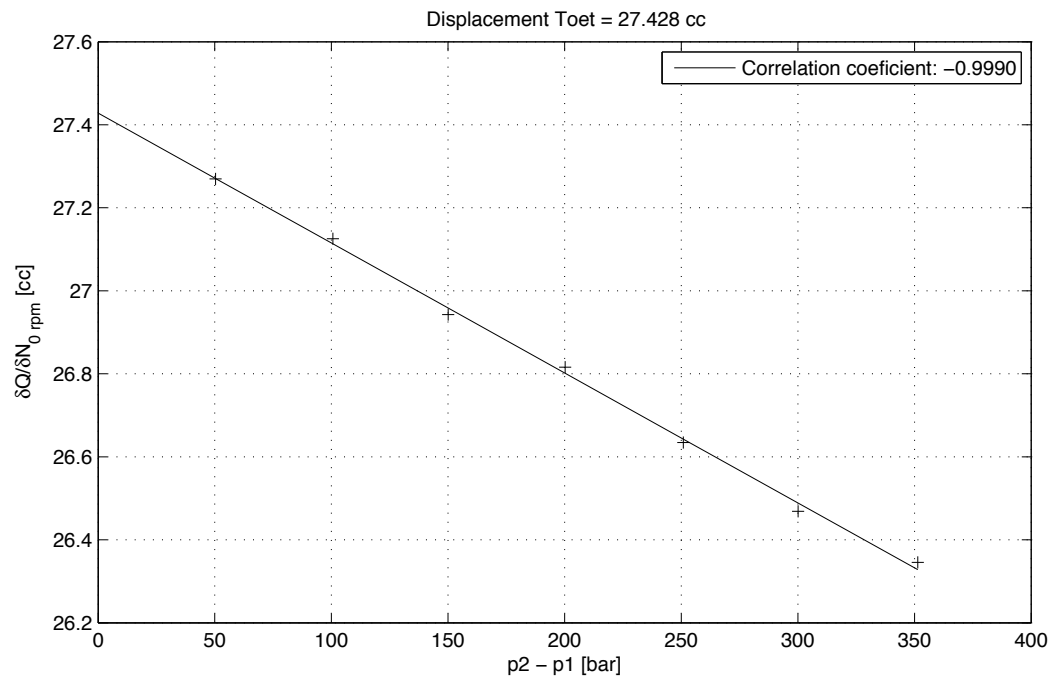


**Figure 4:** *Derived capacity (method Toet) at 8 degrees swash angle*

**Table 1:** *Measured and calculated results at 8 degrees swash-angle*

$\theta_1$ [°C]	$\theta_2$ [°C]	$\theta_{dr}$ [°C]	$n$ [rpm]	$M$ [Nm]	$\Delta p$ [Bar]	$p_1$ [Bar]	$q_{m,2}$ [kg/s]	$q_{dr}$ [Lpm]	$q_{V,1e}$ [Lpm]	$q_{V,2e}$ [Lpm]	$\eta_{tot}$ [%]	$\eta_{hm}$ [%]	$\eta_{vol}$ [%]
39.3	41.5	40.2	504.8	23.46	51.3	3.0	0.20	0.09	13.88	13.70	94.3	95.5	98.9
39.4	41.8	39.4	511.0	45.10	100.8	3.0	0.20	0.17	14.10	13.71	95.4	97.6	97.8
39.4	42.3	40.1	505.3	66.62	150.2	3.0	0.19	0.26	13.98	13.42	95.2	98.5	96.7
39.3	43.0	41.0	505.3	88.24	199.9	3.0	0.19	0.36	14.01	13.24	94.4	99.0	95.5
39.4	43.8	41.9	501.0	110.46	250.9	3.0	0.19	0.48	13.93	12.98	93.5	99.2	94.4
39.4	44.2	43.2	501.4	131.66	299.6	3.0	0.19	0.60	13.98	12.83	92.6	99.4	93.2
39.3	44.8	45.3	498.4	155.04	353.2	3.0	0.18	0.76	13.93	12.57	91.3	99.5	91.8
40.2	46.3	48.6	1001.1	154.76	351.0	3.0	0.38	0.81	27.97	25.83	93.1	99.1	94.0
40.4	46.1	48.5	999.8	132.39	300.0	3.0	0.38	0.67	27.85	25.97	93.6	99.0	94.6
40.4	45.4	47.6	1016.1	110.76	250.4	3.0	0.39	0.54	28.24	26.70	94.5	98.8	95.7
40.1	44.0	46.2	1010.2	89.05	200.5	3.0	0.39	0.41	28.01	26.83	95.1	98.4	96.8
40.2	43.7	45.4	1016.8	67.00	149.7	3.0	0.39	0.30	28.11	27.23	95.2	97.6	97.6
39.7	42.4	44.2	1001.1	45.59	100.4	3.0	0.39	0.19	27.61	27.03	94.6	96.2	98.4
39.8	42.0	43.3	1004.3	24.32	51.4	3.0	0.39	0.10	27.62	27.36	91.6	92.3	99.3
39.5	41.3	41.5	1496.0	24.80	50.2	3.0	0.59	0.11	41.15	40.77	87.8	88.5	99.3
39.5	41.8	42.1	1496.8	46.91	100.9	3.0	0.58	0.21	41.29	40.46	92.4	93.9	98.5
39.5	42.3	43.0	1495.6	68.22	149.8	3.0	0.58	0.31	41.37	40.16	93.8	95.9	97.8
39.6	43.4	43.7	1498.2	90.64	201.6	3.0	0.58	0.43	41.55	39.92	94.3	97.2	97.1
39.4	43.8	44.6	1513.2	111.21	248.8	3.0	0.58	0.55	42.06	40.02	94.1	97.8	96.3
39.9	44.9	45.8	1505.1	133.15	299.4	3.1	0.58	0.68	41.95	39.46	93.8	98.2	95.5
39.8	45.3	47.2	1496.5	155.89	351.8	3.1	0.57	0.83	41.82	38.91	93.3	98.6	94.7
40.2	46.5	49.9	2014.6	155.99	350.2	3.0	0.77	0.94	56.26	52.49	93.0	98.1	94.9
40.6	46.4	51.5	2011.3	133.67	299.4	3.0	0.77	0.81	56.03	52.77	93.5	97.9	95.6
40.8	45.7	51.0	2021.3	111.39	248.1	3.0	0.78	0.65	56.17	53.49	93.7	97.3	96.4
40.9	45.2	49.8	2006.8	93.91	207.8	3.0	0.77	0.54	55.66	53.40	93.7	96.7	96.9
40.8	44.3	49.1	2005.7	69.01	150.2	3.0	0.78	0.38	55.46	53.82	92.9	95.1	97.8
40.9	43.9	48.6	2002.9	47.79	101.4	3.0	0.78	0.26	55.23	54.17	91.3	92.7	98.5
40.7	42.9	48.0	1995.7	25.67	50.4	3.0	0.78	0.14	54.88	54.39	85.1	85.8	99.3
40.4	42.3	47.4	2503.5	26.77	50.4	3.0	0.98	0.17	68.86	68.24	81.7	82.3	99.3
39.8	42.1	47.8	2502.8	48.38	99.9	3.1	0.98	0.28	69.05	67.76	88.9	90.2	98.6
39.9	43.1	48.1	2493.9	69.82	149.2	3.1	0.97	0.41	68.97	67.05	91.4	93.3	97.9
39.7	43.5	49.0	2503.9	91.42	199.0	3.1	0.97	0.55	69.42	66.84	92.4	95.1	97.3
40.0	44.5	50.2	2489.9	114.58	252.7	3.1	0.96	0.70	69.23	65.97	92.9	96.3	96.5
40.0	45.2	51.4	2501.6	135.28	300.5	3.1	0.96	0.86	69.72	65.77	92.9	97.0	95.8
40.4	46.3	53.2	2510.0	157.00	350.7	3.1	0.96	1.05	70.12	65.58	92.8	97.6	95.2
40.4	46.6	55.9	2990.5	152.27	337.5	3.1	1.14	1.14	83.47	78.31	92.3	96.8	95.4
40.8	46.7	56.7	3015.2	136.71	301.8	3.1	1.16	1.02	84.01	79.35	92.4	96.4	95.9
41.0	46.3	56.6	2997.0	116.13	254.2	3.0	1.15	0.86	83.30	79.46	92.3	95.6	96.6
41.0	45.1	54.9	2983.2	94.46	204.5	3.0	1.15	0.69	82.73	79.57	91.8	94.6	97.2
40.6	43.9	54.2	2998.5	71.50	151.0	3.0	1.17	0.51	82.93	80.59	90.3	92.3	97.9
39.7	42.3	53.1	2990.6	49.50	100.4	3.0	1.17	0.38	82.48	80.98	87.4	88.6	98.6
40.8	42.8	51.6	2986.1	28.32	51.1	3.0	1.17	0.28	82.13	81.25	78.2	78.9	99.1

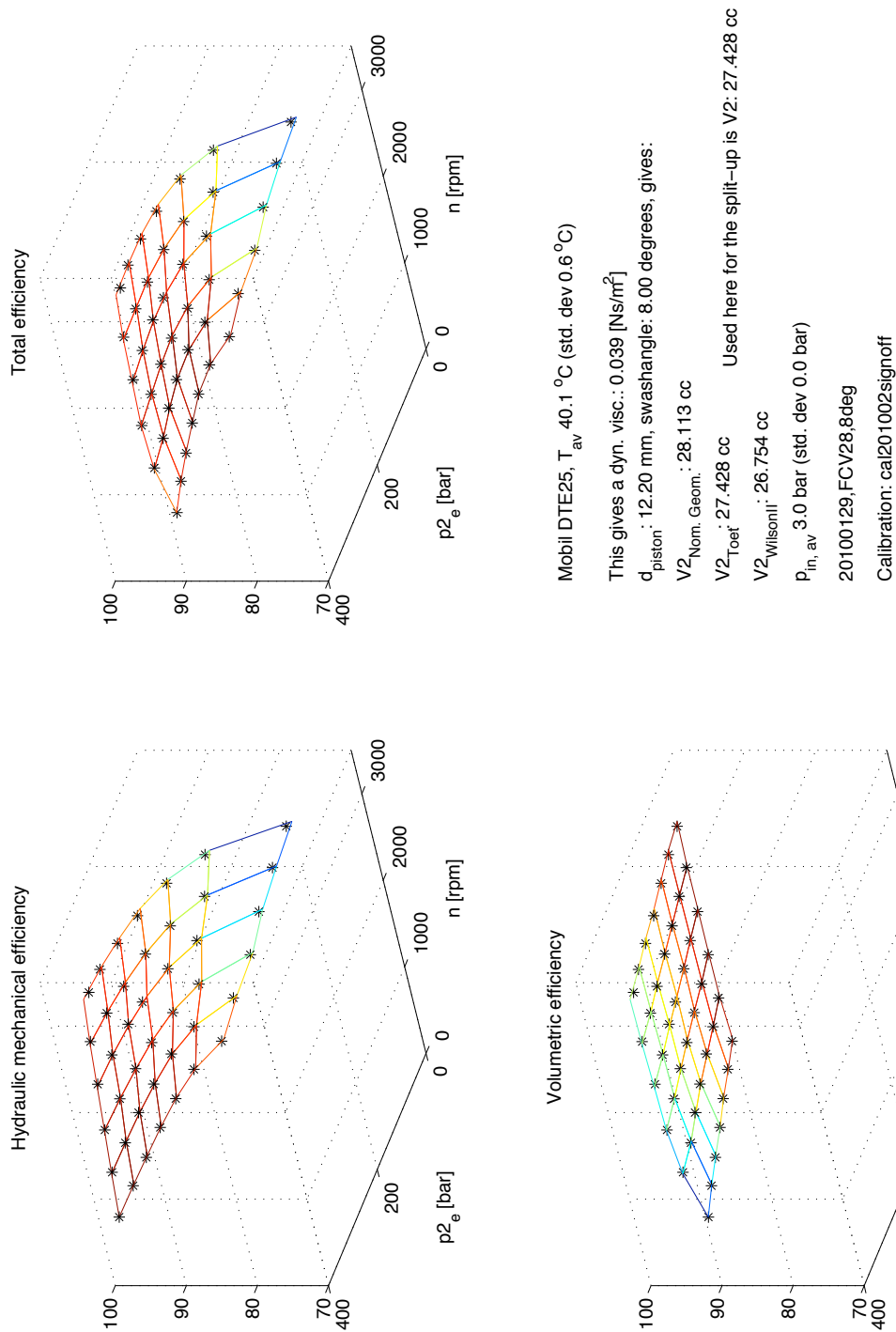
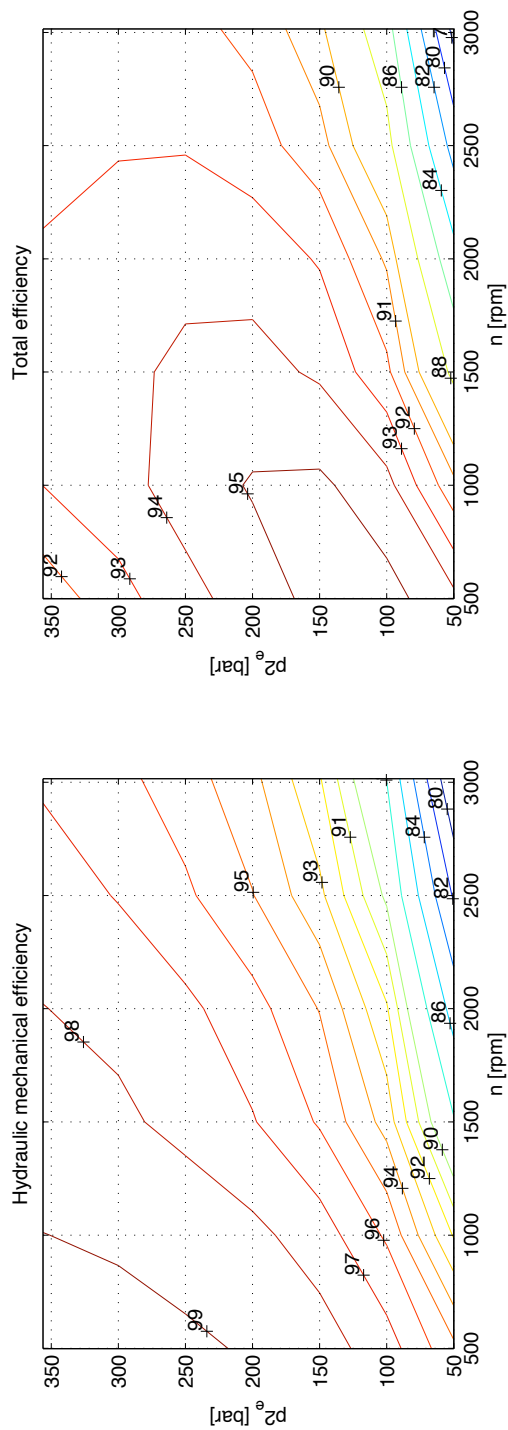


**Figure 5:** Efficiency surface plots, 8 degrees swash angle



Mobil DTE25,  $T_{av}$  40.1 °C (std. dev 0.6 °C)

This gives a dyn. visc.: 0.039 [Ns/m<sup>2</sup>]

$d_{piston}$ : 12.20 mm, swashangle: 8.00 degrees, gives:

$V2_{Nom. Geom.}$ : 28.113 cc

$V2_{Toet}$ : 27.428 cc      Used here for the split-up is  $V2$ : 27.428 cc

$V2_{WilsonI}$ : 26.754 cc

$p_{in, av}$  3.0 bar (std. dev 0.0 bar)

20100129, FCV28.8deg

Calibration: cal201002signoff

**Figure 6:** Efficiency contour plots, 8 degrees swash angle

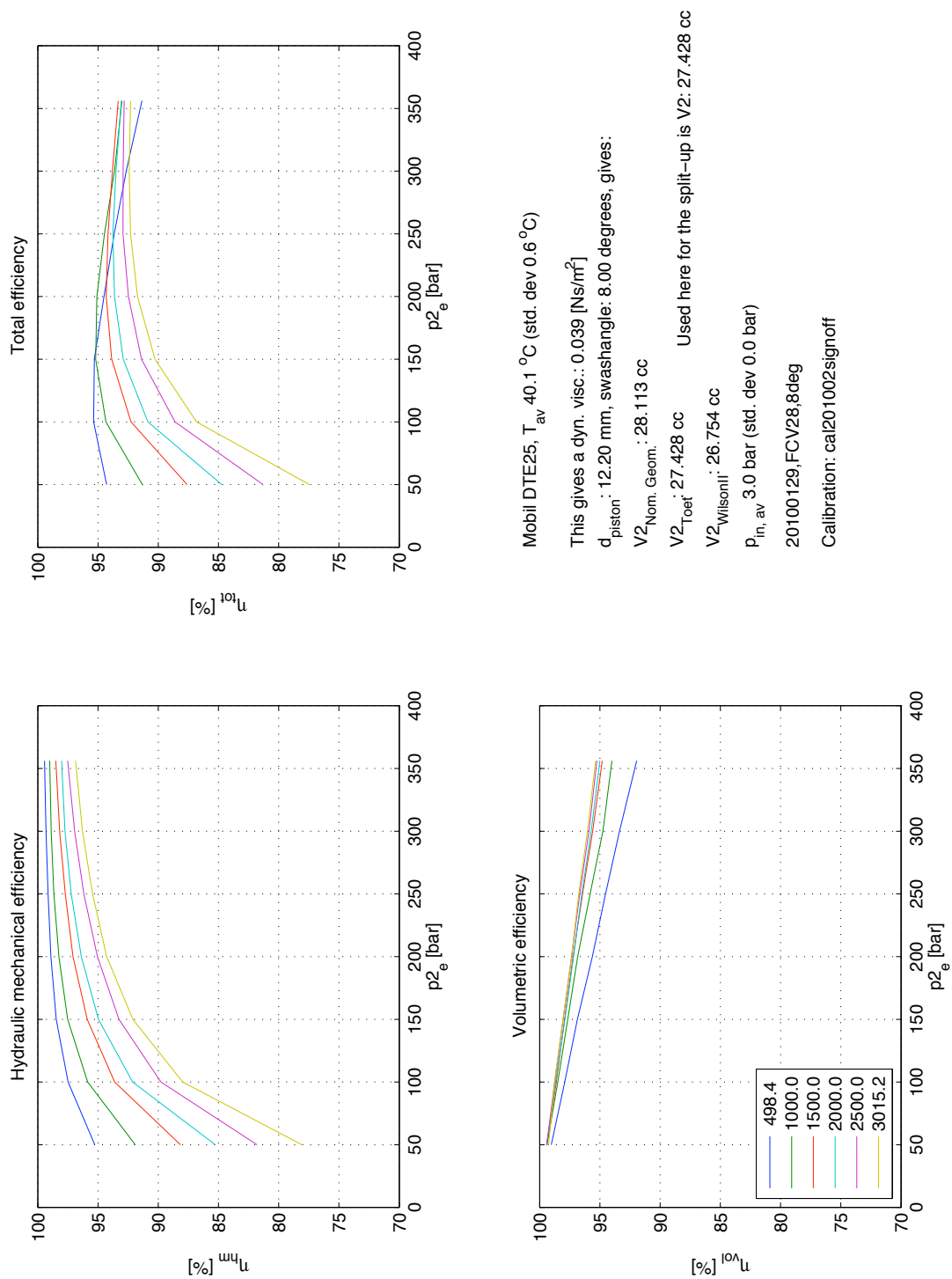


**Figure 7:** Efficiency curves, 8 degrees swash angle

## 8.2 Measurement of the 75% swashed pump (swash-angle: 6 degrees)

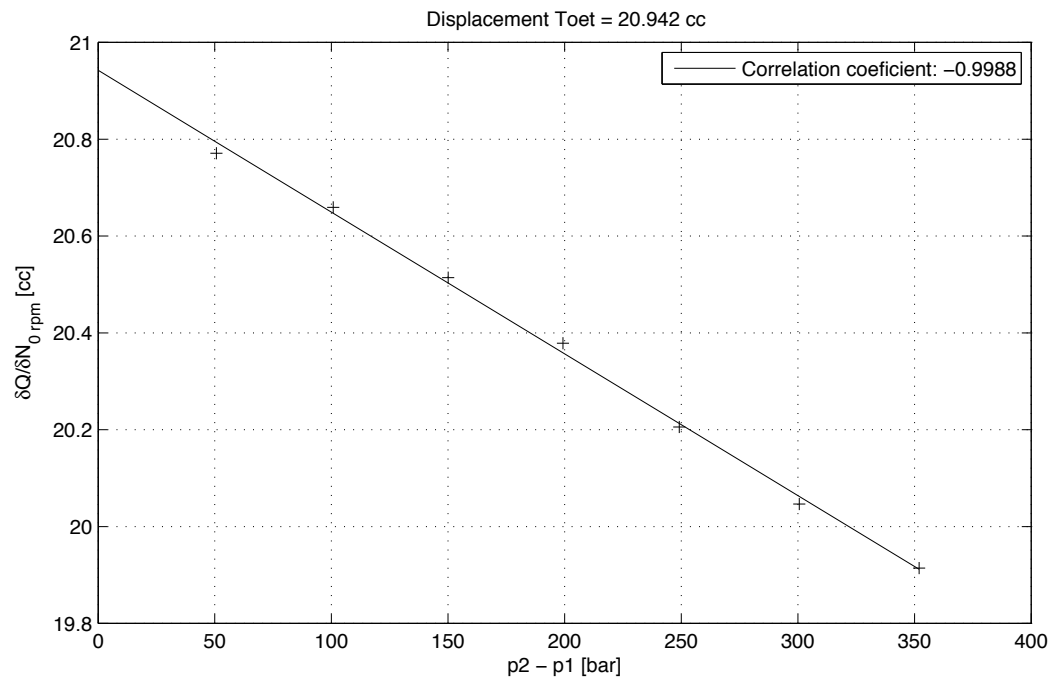
Date: 29-jan-2010

### Properties of Test fluid:

Test fluid:	Mobil	DTE 25
Temperature at inlet:	40.1	[°C] ( $\pm 1.0$ [°C] for all measurements)
Kinematic viscosity:	45.4	[cSt] (or [mm <sup>2</sup> /s])
Density:	861.1	[kg/m <sup>3</sup> ] @ atmospheric conditions and inlet temperature
Inlet pressure:	3.0	[Bar] ( $\pm 1.6$ [%] for all measurements)

### Derived capacity:

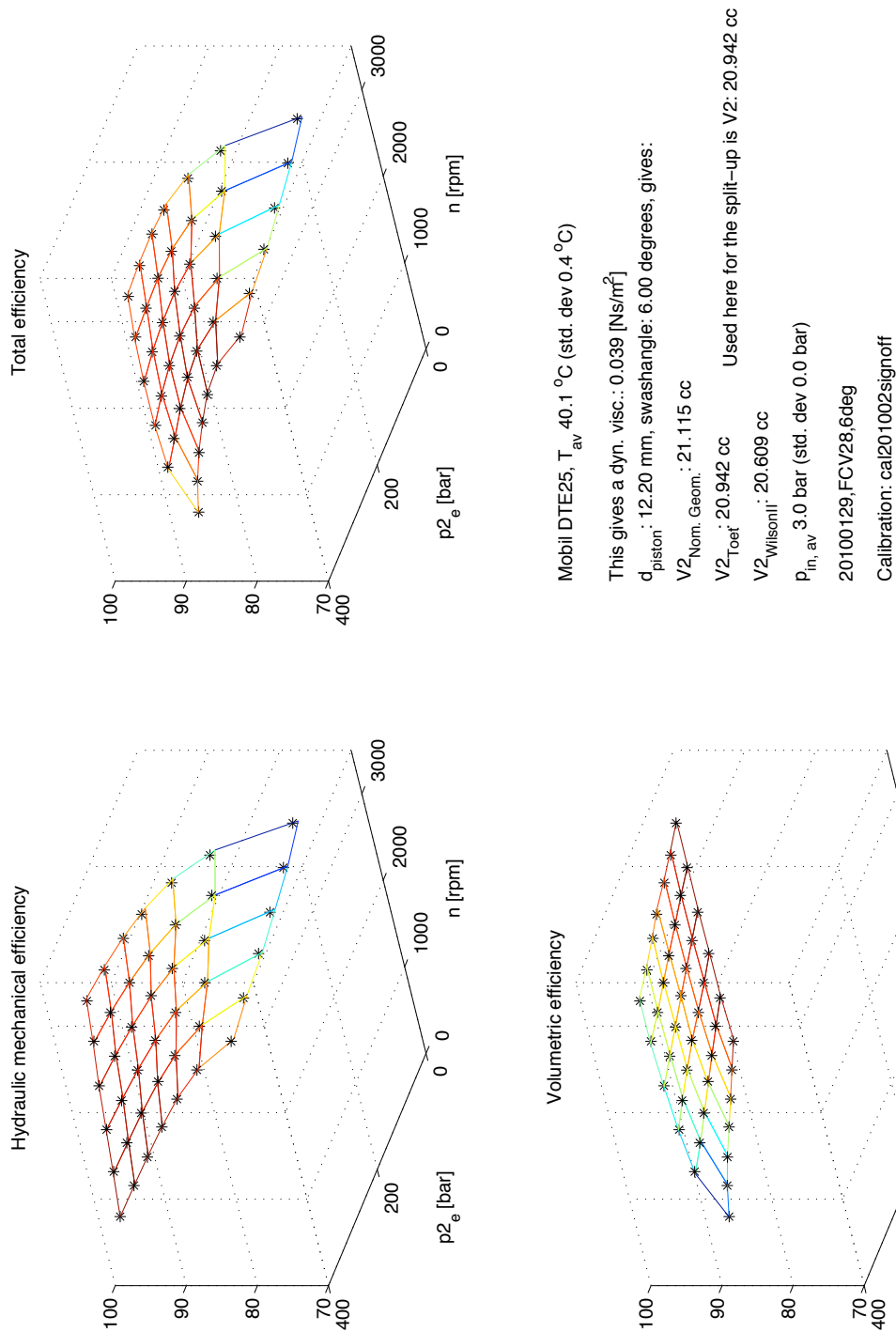
Nominal:	21.12	[cm <sup>3</sup> ]
Toet:	20.94	[cm <sup>3</sup> ]



**Figure 8:** *Derived capacity (method Toet) at 6 degrees swash angle*

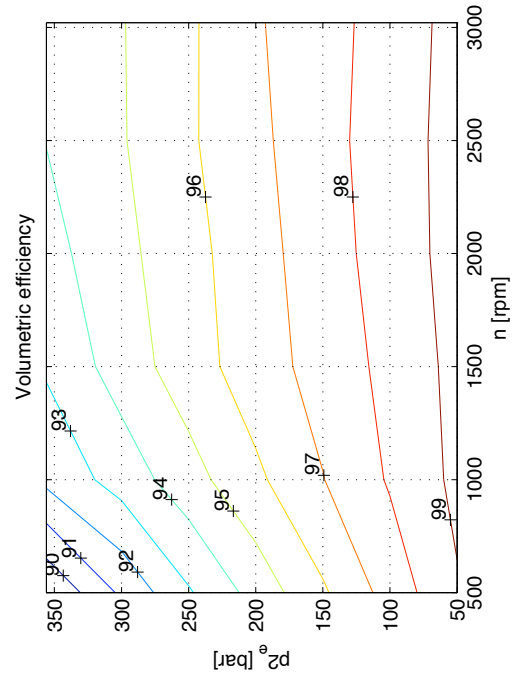
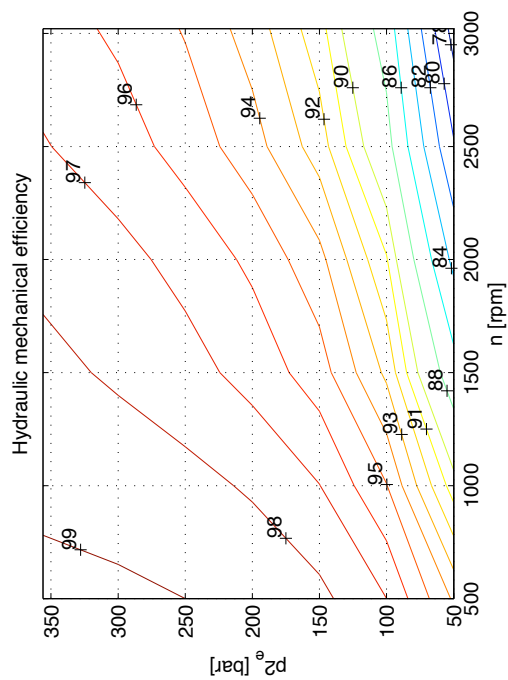
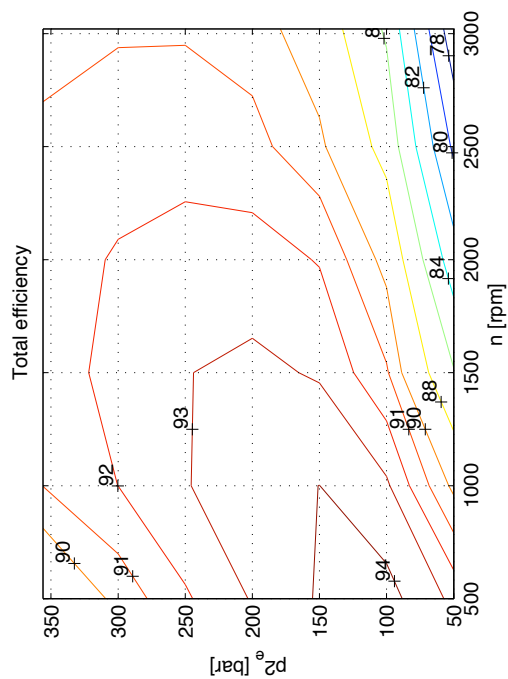
**Table 2:** *Measured and calculated results at 6 degrees swash-angle*

$\theta_1$ [°C]	$\theta_2$ [°C]	$\theta_{dr}$ [°C]	$n$ [rpm]	$M$ [Nm]	$\Delta p$ [Bar]	$p_1$ [Bar]	$q_{m,2}$ [kg/s]	$q_{dr}$ [Lpm]	$q_{V,1e}$ [Lpm]	$q_{V,2e}$ [Lpm]	$\eta_{tot}$ [%]	$\eta_{hm}$ [%]	$\eta_{vol}$ [%]
39.1	41.5	36.8	502.5	18.18	51.3	3.0	0.15	0.09	10.57	10.39	92.8	94.3	98.5
39.3	42.0	38.2	502.7	34.54	100.7	3.0	0.15	0.19	10.61	10.24	94.4	97.4	97.0
39.5	42.9	39.5	501.0	51.01	150.4	3.0	0.15	0.29	10.60	10.05	94.0	98.5	95.5
39.7	43.7	40.6	505.5	67.26	199.2	3.0	0.14	0.39	10.72	9.98	93.0	99.0	94.0
39.7	44.4	42.4	501.1	84.22	250.2	3.0	0.14	0.52	10.66	9.74	91.7	99.3	92.5
39.7	45.1	44.2	503.1	100.71	299.7	3.0	0.14	0.66	10.73	9.60	90.2	99.5	90.8
39.9	46.1	47.0	503.2	118.47	353.0	3.0	0.14	0.84	10.75	9.38	88.3	99.6	88.7
40.1	46.5	48.5	1012.9	118.66	351.5	3.0	0.29	0.86	21.64	19.59	91.1	99.0	92.1
40.3	46.2	49.0	1012.6	102.08	301.9	3.1	0.29	0.72	21.58	19.80	92.0	98.9	93.1
40.4	45.6	48.1	1012.6	84.90	250.5	3.0	0.29	0.58	21.53	20.05	92.9	98.6	94.3
40.3	44.6	46.7	1007.5	66.68	195.8	3.1	0.29	0.43	21.36	20.22	93.7	98.1	95.6
40.0	43.6	45.7	1003.1	51.58	150.2	3.0	0.29	0.32	21.22	20.36	94.0	97.3	96.7
40.0	43.1	45.0	1010.5	35.34	101.0	3.0	0.30	0.21	21.32	20.75	93.4	95.6	97.8
39.8	42.2	44.0	1003.2	18.73	51.0	3.1	0.30	0.10	21.10	20.83	90.0	91.1	98.9
39.9	42.1	43.0	1515.6	19.55	51.1	3.1	0.45	0.12	31.89	31.48	86.4	87.4	98.9
39.8	42.1	43.3	1510.8	36.07	100.7	3.1	0.45	0.22	31.89	31.07	91.3	93.3	97.9
39.9	43.0	43.9	1496.3	52.27	149.7	3.1	0.44	0.34	31.66	30.50	92.8	95.7	97.0
40.1	43.7	44.4	1509.1	68.85	199.6	3.1	0.44	0.46	32.02	30.50	93.2	96.9	96.2
40.2	44.8	45.5	1503.9	85.51	249.8	3.1	0.44	0.60	31.98	30.07	92.9	97.7	95.2
40.2	45.3	46.8	1499.3	102.69	301.5	3.1	0.43	0.74	31.97	29.63	92.3	98.1	94.1
40.2	46.0	48.3	1499.7	119.35	351.8	3.1	0.43	0.91	32.06	29.23	91.4	98.5	92.8
40.2	46.6	51.3	2011.9	120.24	352.6	3.0	0.58	1.03	42.99	39.45	91.4	98.0	93.4
40.7	46.9	52.3	2005.1	102.97	300.8	3.0	0.58	0.86	42.73	39.74	92.1	97.6	94.4
40.3	45.5	51.6	1999.8	86.01	249.6	3.0	0.58	0.69	42.51	40.03	92.4	97.0	95.3
40.8	45.4	50.5	2006.6	68.51	196.9	3.0	0.59	0.53	42.54	40.60	92.5	96.1	96.3
40.5	44.2	49.6	2010.8	53.17	150.6	3.0	0.59	0.39	42.53	41.05	91.9	94.6	97.2
40.8	44.1	48.9	1998.6	36.69	100.8	3.0	0.59	0.26	42.15	41.18	90.0	91.8	98.1
40.2	42.0	48.0	1993.4	20.35	51.3	3.0	0.60	0.13	41.95	41.45	83.5	84.3	99.0
40.0	42.1	47.2	2506.4	20.92	50.7	3.0	0.75	0.16	52.73	52.11	80.1	80.9	99.0
39.7	42.1	47.8	2515.1	37.47	100.1	3.0	0.75	0.28	53.08	51.88	87.6	89.3	98.2
39.6	42.7	48.1	2505.0	53.74	149.1	3.0	0.74	0.42	53.00	51.20	90.2	92.8	97.3
40.0	44.0	49.2	2499.6	71.06	201.4	3.1	0.73	0.57	53.02	50.62	91.3	94.7	96.4
40.0	44.6	50.5	2497.5	86.26	247.4	3.0	0.73	0.73	53.10	50.14	91.6	95.9	95.6
40.5	45.9	52.2	2506.0	103.69	300.1	3.1	0.73	0.92	53.42	49.79	91.5	96.7	94.6
40.3	46.1	53.6	2508.4	120.20	350.0	3.1	0.72	1.12	53.61	49.40	91.2	97.3	93.8
40.9	47.7	57.0	2996.0	121.95	353.0	3.0	0.86	1.31	64.01	59.00	90.7	96.7	93.8
41.0	47.0	57.7	2994.0	104.13	299.5	3.1	0.87	1.08	63.80	59.50	90.9	96.1	94.6
40.9	45.8	56.6	3009.3	86.88	247.4	3.0	0.88	0.86	63.98	60.38	90.9	95.2	95.5
40.4	44.5	56.0	3007.9	73.15	205.8	3.0	0.88	0.69	63.82	60.93	90.7	94.0	96.5
39.6	43.2	54.7	3000.1	54.78	150.4	3.0	0.89	0.50	63.46	61.29	89.2	91.7	97.3
39.5	42.7	53.7	2991.4	38.50	101.4	3.0	0.89	0.35	63.10	61.62	86.3	88.1	98.1
39.7	42.4	53.1	3020.4	21.76	50.8	3.0	0.90	0.22	63.53	62.79	77.2	78.0	99.0



**Figure 9:** Efficiency surface plots, 6 degrees swash angle



Mobil DTE25,  $T_{av}$  40.1 °C (std. dev 0.4 °C)

This gives a dyn. visc.:  $0.039 \text{ [Ns/m}^2\text{]}$

$d_{\text{piston}}$ : 12.20 mm, swashangle: 6.00 degrees, gives:

V2<sub>Nom. Geom.</sub>: 21.115 cc

V2<sub>Toet</sub>: 20.942 cc

V2<sub>WilsonII</sub>: 20.609 cc

$p_{in,av}$  3.0 bar (std. dev 0.0 bar)

III, av  
20100129,FCV28,6deg

Calibration: cal201002signoff

Used here for the split-up is V2: 20.942 cc

**Figure 10:** *Efficiency contour plots, 6 degrees swash angle*

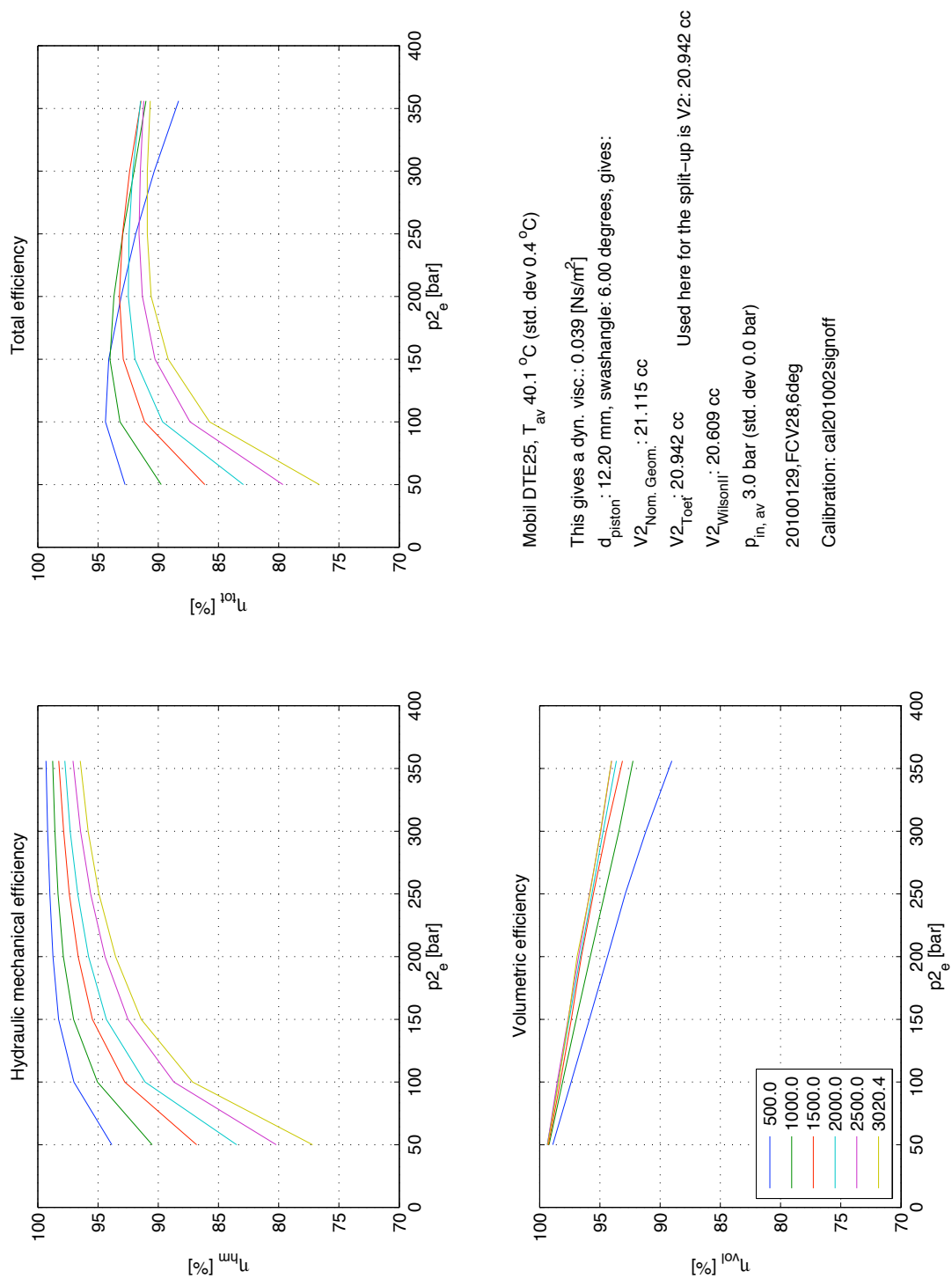


**Figure 11:** Efficiency curves, 6 degrees swash angle

### 8.3 Measurement of the 50% swashed pump (swash-angle: 4 degrees)

Date: 29-jan-2010

#### Properties of Test fluid:

Test fluid:	Mobil	DTE 25
Temperature at inlet:	40.1	[°C] ( $\pm 0.8$ [°C] for all measurements)
Kinematic viscosity:	45.3	[cSt] (or [mm <sup>2</sup> /s])
Density:	861.0	[kg/m <sup>3</sup> ] @ atmospheric conditions and inlet temperature
Inlet pressure:	3.0	[Bar] ( $\pm 3.0$ [%] for all measurements)

#### Derived capacity:

Nominal:	14.09	[cm <sup>3</sup> ]
Toet:	13.74	[cm <sup>3</sup> ]

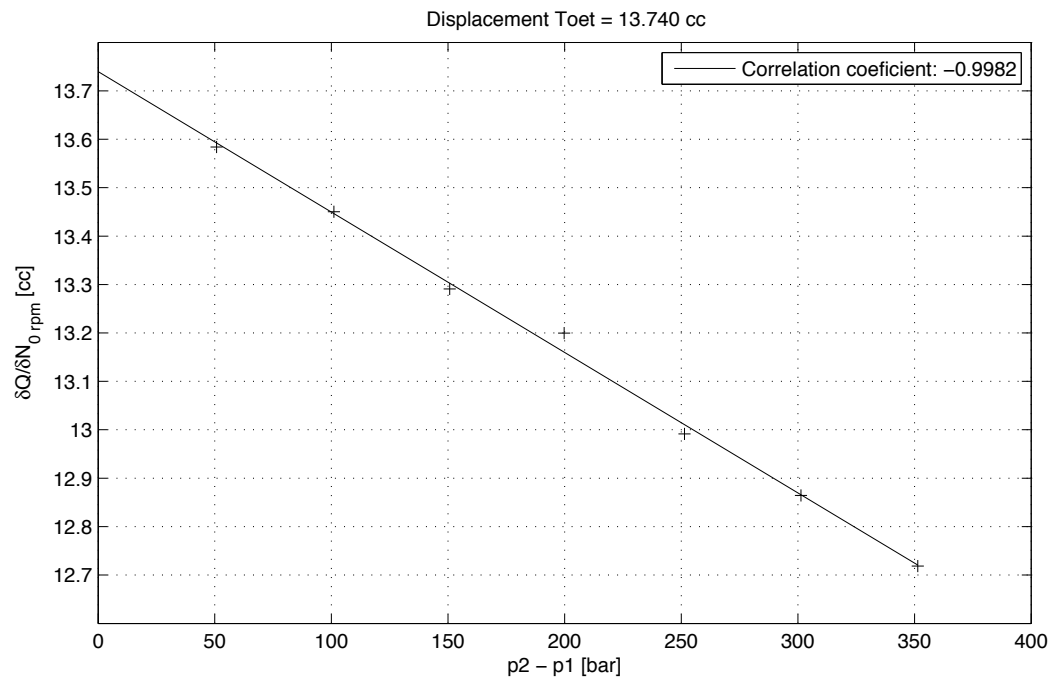
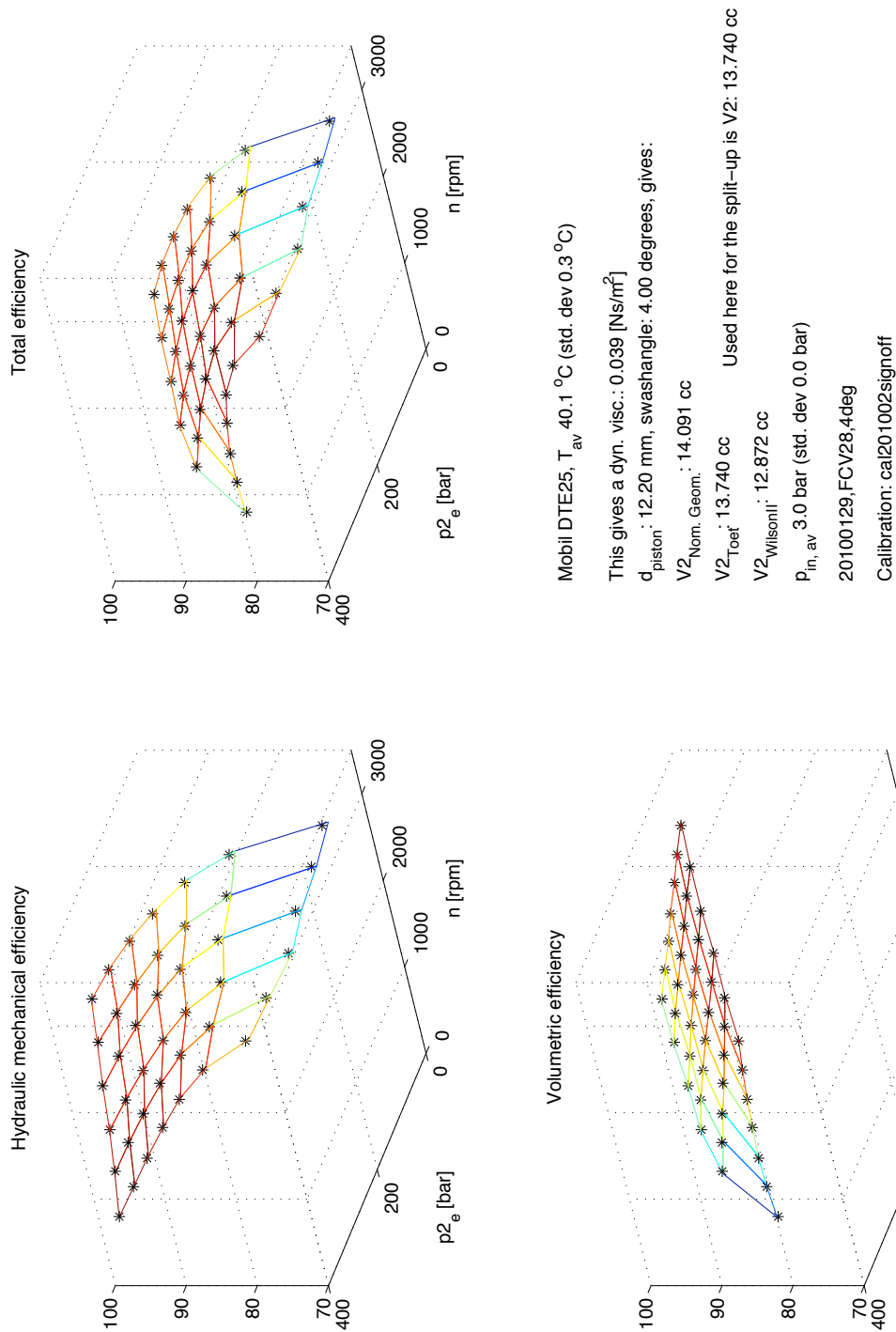


Figure 12: Derived capacity (method Toet) at 4 degrees swash angle

**Table 3:** *Measured and calculated results at 4 degrees swash-angle*

$\theta_1$ [°C]	$\theta_2$ [°C]	$\theta_{dr}$ [°C]	$n$ [rpm]	$M$ [Nm]	$\Delta p$ [Bar]	$p_1$ [Bar]	$q_{m,2}$ [kg/s]	$q_{dr}$ [Lpm]	$q_{V,1e}$ [Lpm]	$q_{V,2e}$ [Lpm]	$\eta_{tot}$ [%]	$\eta_{hm}$ [%]	$\eta_{vol}$ [%]
40.1	42.7	39.4	506.9	12.18	51.2	3.0	0.10	0.10	7.01	6.83	90.1	92.4	97.6
40.2	43.1	40.2	510.5	23.10	101.7	3.0	0.10	0.20	7.08	6.72	92.1	96.7	95.3
40.2	43.4	40.7	503.1	33.80	151.3	3.0	0.09	0.30	7.00	6.46	91.3	98.4	93.0
40.3	44.4	42.1	507.5	44.44	200.3	3.0	0.09	0.42	7.07	6.34	89.5	99.0	90.6
40.4	45.2	43.7	499.8	55.62	251.8	3.0	0.09	0.57	6.98	6.07	87.3	99.4	87.9
40.4	45.9	45.9	504.3	66.50	301.7	3.0	0.09	0.72	7.06	5.92	84.6	99.6	85.1
40.1	46.4	48.6	496.2	77.35	351.8	3.0	0.08	0.90	6.97	5.60	81.6	99.9	81.8
40.0	46.8	50.1	1009.9	77.77	350.5	3.1	0.18	0.94	14.17	12.28	87.1	99.0	88.1
40.2	46.7	50.1	1015.2	67.03	301.7	3.1	0.18	0.79	14.21	12.58	88.7	98.8	89.8
40.4	46.2	49.2	1007.1	56.02	251.2	3.1	0.18	0.63	14.07	12.73	90.1	98.5	91.6
40.4	45.4	48.0	1024.6	45.19	201.2	3.1	0.19	0.49	14.27	13.17	91.0	97.8	93.1
40.3	44.4	46.9	1005.8	34.06	150.0	3.1	0.19	0.34	13.98	13.16	91.6	96.7	94.8
40.2	43.6	46.0	1006.5	23.58	101.2	3.1	0.19	0.22	13.95	13.39	90.8	94.3	96.4
40.0	42.6	44.7	1006.2	12.78	51.2	3.1	0.20	0.11	13.91	13.62	86.2	88.0	98.1
39.9	42.2	43.7	1516.3	13.39	50.8	3.1	0.30	0.12	20.96	20.53	81.6	83.3	98.1
39.9	42.6	44.2	1518.0	24.30	100.9	3.0	0.29	0.24	21.05	20.25	88.0	91.2	96.7
39.9	43.2	44.8	1505.7	35.13	151.0	3.1	0.29	0.36	20.93	19.82	90.0	94.4	95.4
39.9	43.8	45.1	1504.3	45.64	199.4	3.1	0.28	0.50	20.97	19.56	90.3	95.9	94.2
39.9	44.6	46.4	1504.3	56.77	250.7	3.1	0.28	0.65	21.02	19.26	89.9	97.0	92.8
40.2	45.7	48.0	1507.4	67.86	301.9	3.1	0.28	0.82	21.12	19.00	89.1	97.7	91.3
40.4	46.9	50.2	1499.7	78.65	351.7	3.1	0.27	1.03	21.06	18.53	87.9	98.2	89.6
40.5	47.4	52.7	2014.5	79.43	353.1	3.0	0.36	1.16	28.28	24.96	87.6	97.6	89.8
40.7	47.2	53.2	2009.6	67.97	300.9	3.0	0.37	0.96	28.13	25.34	88.7	97.2	91.4
40.5	46.0	52.3	2024.8	57.04	250.6	3.0	0.38	0.76	28.28	25.97	89.6	96.5	92.9
40.6	45.5	51.3	2017.5	45.40	197.0	3.0	0.38	0.58	28.10	26.29	89.9	95.3	94.4
40.3	44.0	50.1	1998.6	35.20	150.2	3.1	0.38	0.42	27.78	26.41	89.6	93.7	95.7
40.4	43.6	49.4	2005.8	24.51	100.5	3.0	0.39	0.28	27.80	26.87	87.3	90.1	97.1
40.1	42.5	48.7	2007.5	13.94	51.3	3.0	0.39	0.15	27.75	27.26	79.5	80.8	98.4
40.2	42.6	48.3	2513.9	14.42	50.6	3.0	0.49	0.17	34.75	34.14	75.8	77.1	98.4
40.2	42.9	48.9	2512.0	25.35	100.8	3.0	0.49	0.31	34.83	33.69	84.8	87.3	97.2
40.3	43.6	49.3	2501.7	36.18	150.8	3.0	0.48	0.46	34.78	33.09	87.6	91.5	95.9
40.1	44.0	50.4	2501.5	47.14	201.0	3.0	0.47	0.62	34.87	32.65	88.5	93.7	94.6
40.1	44.8	51.4	2511.7	58.45	253.0	3.1	0.47	0.81	35.10	32.31	88.5	95.1	93.2
39.8	45.2	52.7	2499.1	68.74	300.5	3.1	0.46	1.00	35.01	31.72	88.2	96.0	92.0
39.9	46.5	54.4	2498.5	79.32	350.0	3.1	0.46	1.25	35.07	31.17	87.5	96.9	90.4
39.8	46.7	56.2	3004.4	80.14	351.0	3.0	0.55	1.44	42.17	37.55	87.0	96.2	90.6
40.3	47.1	57.9	3008.0	69.25	301.4	3.0	0.56	1.21	42.11	38.13	87.7	95.6	91.8
40.2	45.6	57.1	3001.0	58.42	251.1	3.0	0.56	0.95	41.92	38.55	87.8	94.4	93.1
39.9	44.7	56.2	3005.9	48.50	204.7	3.0	0.57	0.75	41.89	39.15	87.4	92.7	94.4
39.7	43.7	55.1	3006.4	36.81	150.9	3.0	0.57	0.55	41.78	39.69	86.0	90.0	95.7
39.5	42.7	54.1	2996.1	26.07	101.4	3.0	0.58	0.37	41.53	40.10	82.8	85.5	97.0
39.4	42.1	53.5	2993.4	15.10	50.9	2.9	0.58	0.21	41.37	40.58	72.7	74.1	98.2



**Figure 13:** *Efficiency surface plots, 4 degrees swash angle*

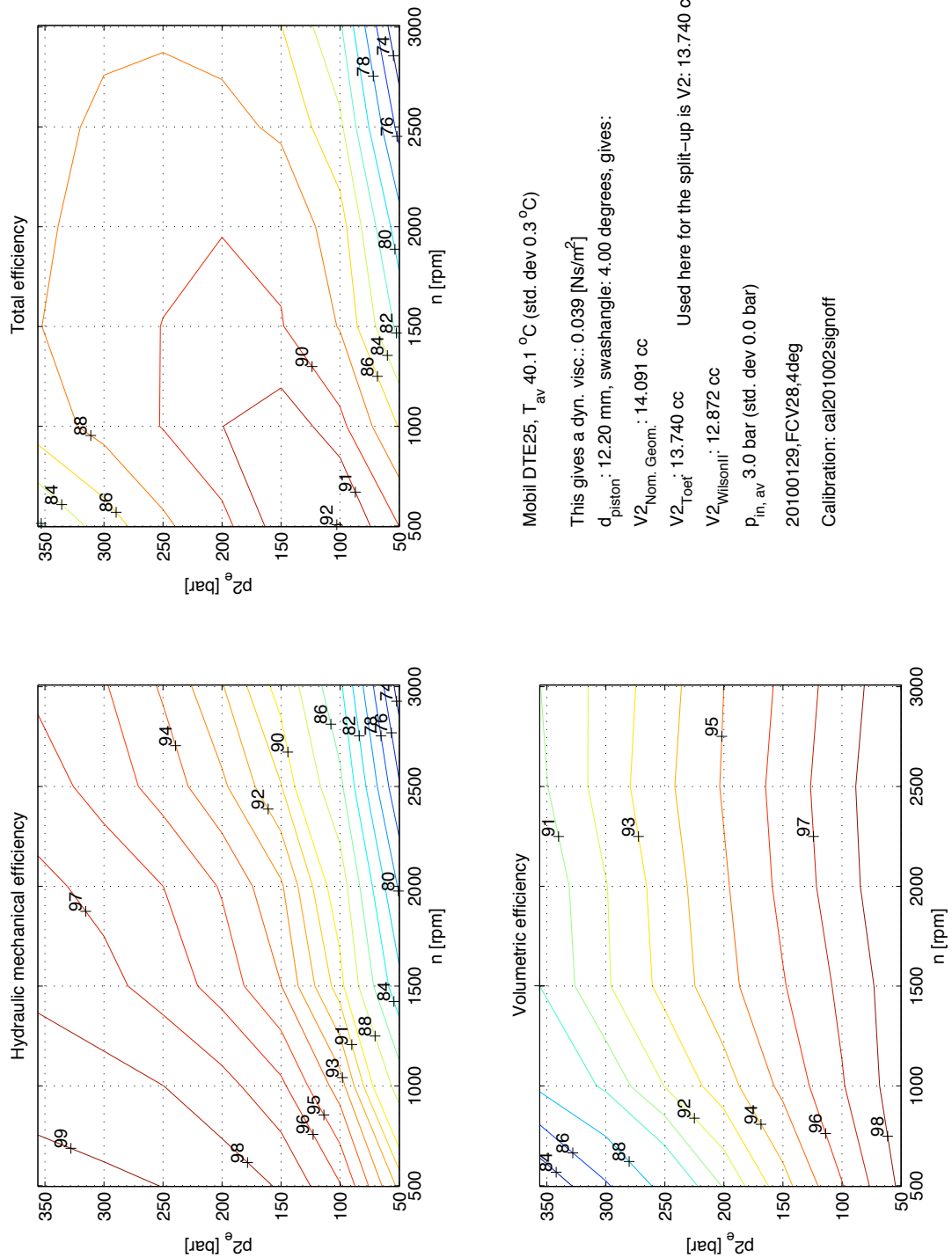


**Figure 14:** *Efficiency contour plots, 4 degrees swash angle*

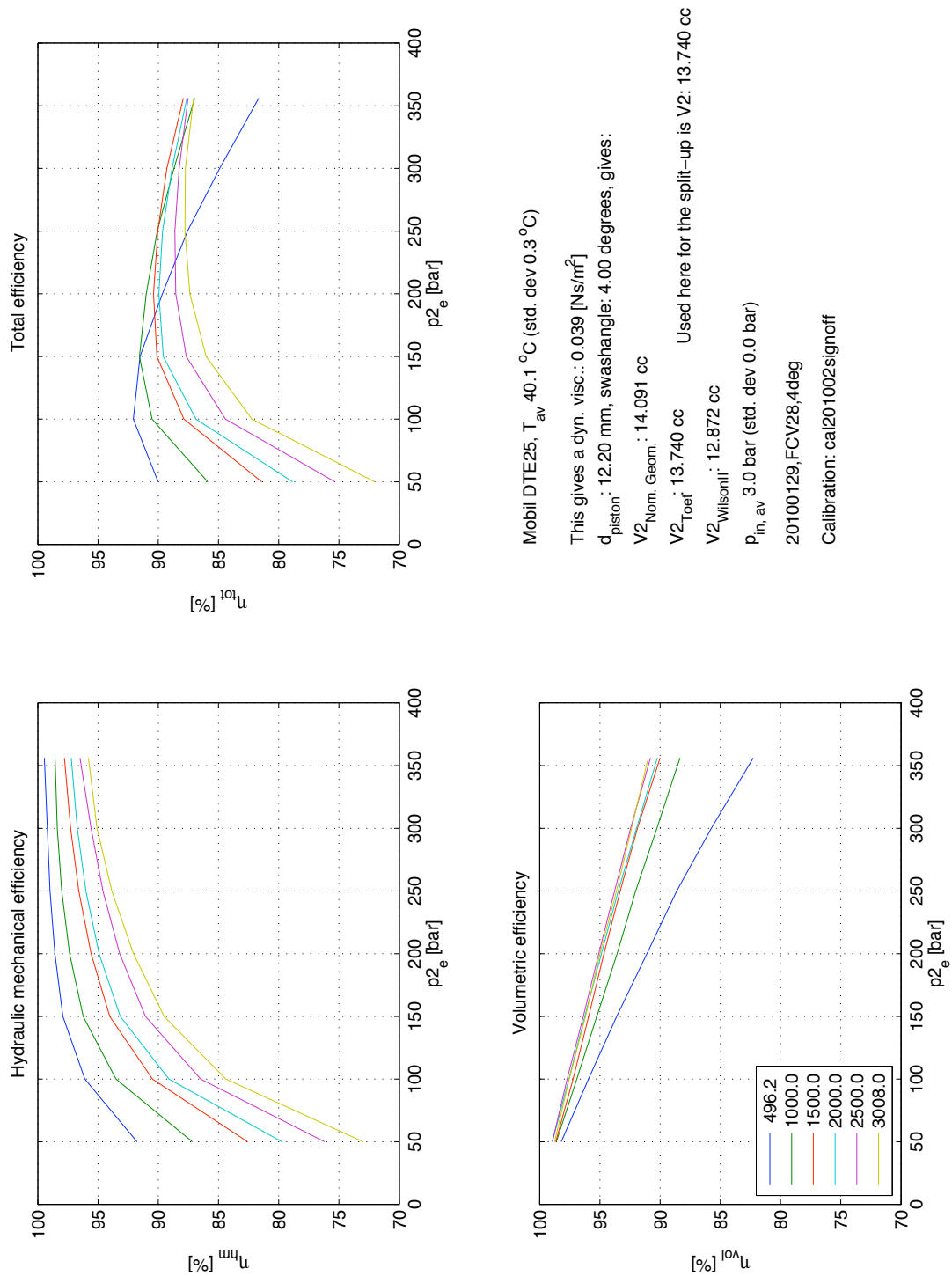


**Figure 15:** Efficiency curves, 4 degrees swash angle

## 8.4 Measurement of the 25% swashed pump (swash-angle: 2 degrees)

Date: 01-Feb-2010

### Properties of Test fluid:

Test fluid:	Mobil	DTE 25
Temperature at inlet:	40.3	[°C] ( $\pm 0.6$ [°C] for all measurements)
Kinematic viscosity:	45.0	[cSt] (or [mm <sup>2</sup> /s])
Density:	860.9	[kg/m <sup>3</sup> ] @ atmospheric conditions and inlet temperature
Inlet pressure:	3.0	[Bar] ( $\pm 2.9$ [%] for all measurements)

### Derived capacity:

Nominal:	7.05	[cm <sup>3</sup> ]
Toet:	6.64	[cm <sup>3</sup> ]

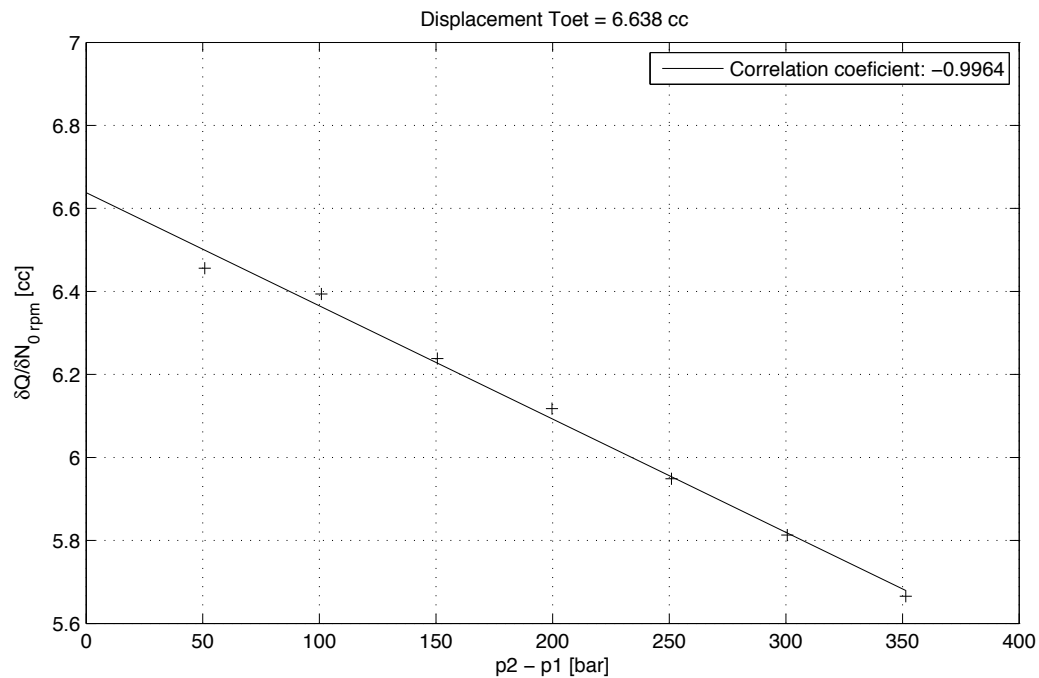


**Figure 16:** *Derived capacity (method Toet) at 2 degrees swash angle*



**Table 4:** *Measured and calculated results at 2 degrees swash-angle*

$\theta_1$ [°C]	$\theta_2$ [°C]	$\theta_{dr}$ [°C]	$n$ [rpm]	$M$ [Nm]	$\Delta p$ [Bar]	$p_1$ [Bar]	$q_{m,2}$ [kg/s]	$q_{dr}$ [Lpm]	$q_{V,1e}$ [Lpm]	$q_{V,2e}$ [Lpm]	$\eta_{tot}$ [%]	$\eta_{hm}$ [%]	$\eta_{vol}$ [%]
40.3	43.4	39.0	500.4	6.58	51.3	3.1	0.05	0.10	3.34	3.19	79.0	82.6	95.8
40.5	43.9	40.7	497.2	11.67	100.7	3.1	0.04	0.21	3.33	3.01	82.9	91.4	90.9
40.3	43.9	41.7	499.7	16.90	150.7	3.1	0.04	0.33	3.35	2.86	81.1	94.5	86.0
40.2	44.5	42.8	505.9	22.06	199.6	3.1	0.04	0.46	3.40	2.73	77.3	95.9	80.9
40.1	45.4	44.9	512.9	27.44	250.4	3.1	0.04	0.61	3.46	2.57	72.6	96.7	75.3
40.2	46.5	48.0	503.8	32.59	299.2	3.1	0.03	0.79	3.40	2.29	66.2	97.3	68.4
40.4	48.0	52.7	505.0	37.84	349.0	3.1	0.03	1.02	3.42	2.02	58.3	97.8	60.0
40.8	49.1	54.6	1003.6	38.80	351.2	3.0	0.07	1.12	6.79	4.92	70.3	95.9	73.5
40.9	49.0	54.3	1002.4	33.40	300.9	3.0	0.08	0.93	6.77	5.19	73.9	95.5	77.7
40.7	48.2	53.0	1006.8	28.15	251.7	3.0	0.08	0.75	6.78	5.50	77.5	94.8	82.0
40.6	46.9	51.2	1002.5	22.65	199.9	3.0	0.08	0.56	6.73	5.73	80.1	93.6	85.9
40.4	45.6	49.3	1004.3	17.44	150.3	3.0	0.09	0.39	6.73	6.02	82.1	91.4	90.1
40.2	44.5	48.0	999.8	12.34	101.1	3.0	0.09	0.25	6.68	6.23	81.0	86.9	93.5
40.0	43.6	46.8	1008.0	7.14	51.3	3.0	0.09	0.12	6.72	6.52	73.8	76.1	97.1
39.9	42.9	45.4	1556.5	7.76	50.9	3.0	0.15	0.14	10.38	10.13	67.8	69.5	97.8
39.8	43.0	45.9	1516.5	12.97	100.6	3.1	0.14	0.26	10.14	9.56	77.7	82.2	94.7
39.8	43.6	46.1	1504.2	18.22	150.9	3.1	0.13	0.40	10.09	9.20	80.5	87.8	91.8
39.9	44.3	46.5	1505.1	23.40	200.1	3.1	0.13	0.56	10.12	8.91	80.4	90.6	88.9
40.1	45.4	48.0	1485.3	28.70	250.5	3.1	0.12	0.74	10.01	8.46	79.0	92.5	85.6
40.2	46.7	50.2	1514.2	34.14	301.8	3.1	0.12	0.97	10.23	8.23	76.3	93.7	81.6
40.2	47.8	52.8	1495.7	39.28	351.4	3.1	0.11	1.20	10.13	7.66	72.7	94.8	76.9
40.4	48.9	55.3	1997.0	39.88	352.6	3.0	0.15	1.39	13.52	10.54	74.1	93.7	79.2
40.5	48.7	56.4	1988.0	34.31	300.6	3.0	0.16	1.13	13.42	10.93	76.5	92.9	82.6
40.7	48.1	55.9	2024.2	29.17	251.7	3.0	0.17	0.91	13.63	11.58	78.4	91.4	85.9
40.5	46.8	54.5	1996.1	23.79	200.7	3.0	0.17	0.67	13.41	11.83	79.4	89.4	89.0
40.5	46.0	53.1	1997.6	18.46	150.2	3.0	0.18	0.49	13.38	12.22	79.1	86.3	91.9
40.4	44.8	52.0	2007.2	13.33	100.9	3.0	0.18	0.31	13.42	12.67	76.0	80.3	94.8
40.3	43.9	51.0	2011.0	8.10	50.8	2.9	0.19	0.16	13.41	13.07	64.8	66.5	97.6
40.2	43.2	50.5	2500.6	8.78	51.3	3.1	0.23	0.19	16.68	16.27	60.4	61.9	97.7
40.1	43.6	50.8	2513.8	14.05	101.2	3.0	0.23	0.34	16.81	15.96	72.7	76.4	95.3
40.2	44.1	51.1	2500.2	19.28	150.7	3.1	0.22	0.51	16.77	15.39	76.5	82.9	92.4
40.1	44.8	52.2	2502.5	24.50	200.2	3.1	0.22	0.70	16.83	14.94	77.5	86.6	89.6
39.9	46.1	52.6	2525.1	29.82	250.8	3.1	0.21	0.92	17.01	14.63	77.4	89.2	87.0
40.0	46.7	54.8	2518.7	35.06	301.2	3.1	0.20	1.18	17.02	14.08	76.2	91.1	83.9
40.2	48.3	57.7	2503.1	40.32	351.7	3.1	0.20	1.53	16.94	13.46	74.5	92.5	80.8
40.3	49.0	60.8	3020.8	40.98	352.3	3.0	0.24	1.73	20.44	16.23	73.4	91.1	80.7
40.5	49.0	61.3	3039.5	35.41	300.1	3.0	0.25	1.42	20.51	17.00	75.3	89.8	84.0
40.4	47.7	60.3	3011.9	30.17	250.5	3.0	0.25	1.11	20.28	17.40	76.2	88.0	86.7
40.6	46.8	59.5	3010.1	24.66	197.9	3.0	0.26	0.83	20.22	18.05	76.4	85.0	90.0
40.4	45.6	57.9	3011.1	19.66	150.4	3.0	0.27	0.62	20.18	18.52	74.8	81.1	92.3
40.5	44.8	56.9	3005.9	14.38	100.6	3.0	0.27	0.42	20.09	19.03	70.4	74.2	95.0
40.6	44.4	56.5	3013.0	9.23	51.1	3.0	0.28	0.24	20.08	19.63	57.3	58.6	97.8

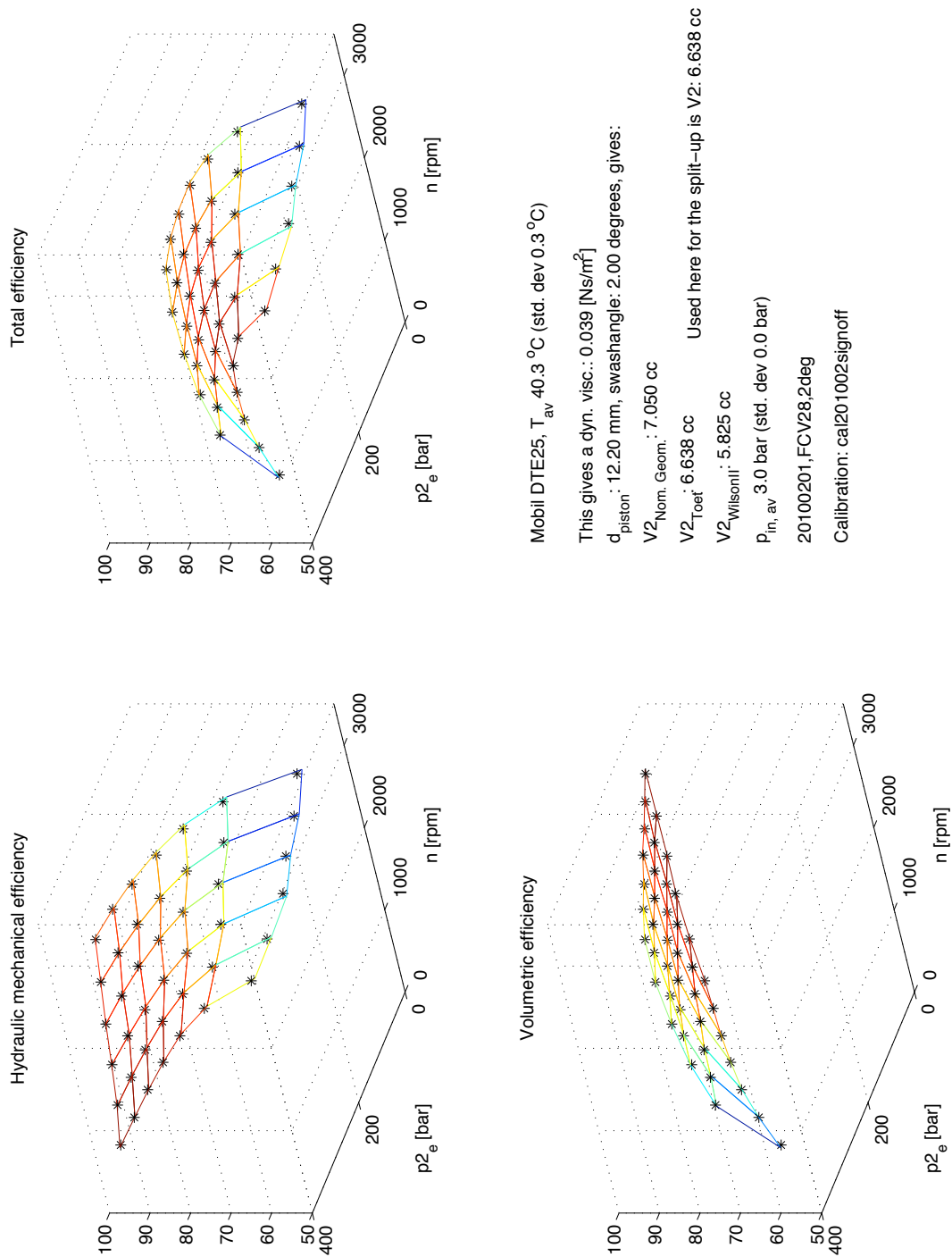


**Figure 17:** Efficiency surface plots, 2 degrees swash angle

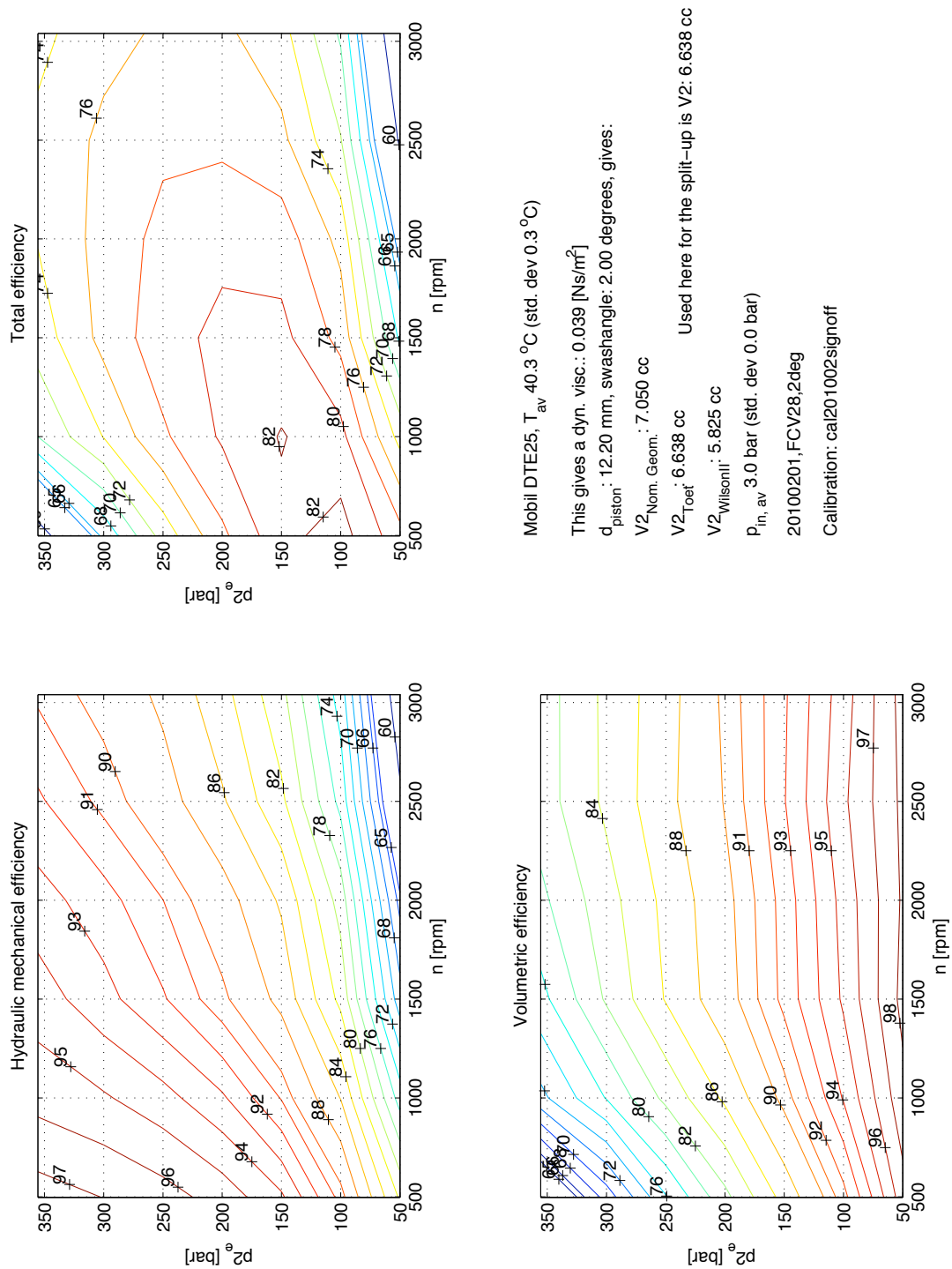


**Figure 18:** *Efficiency contour plots, 2 degrees swash angle*

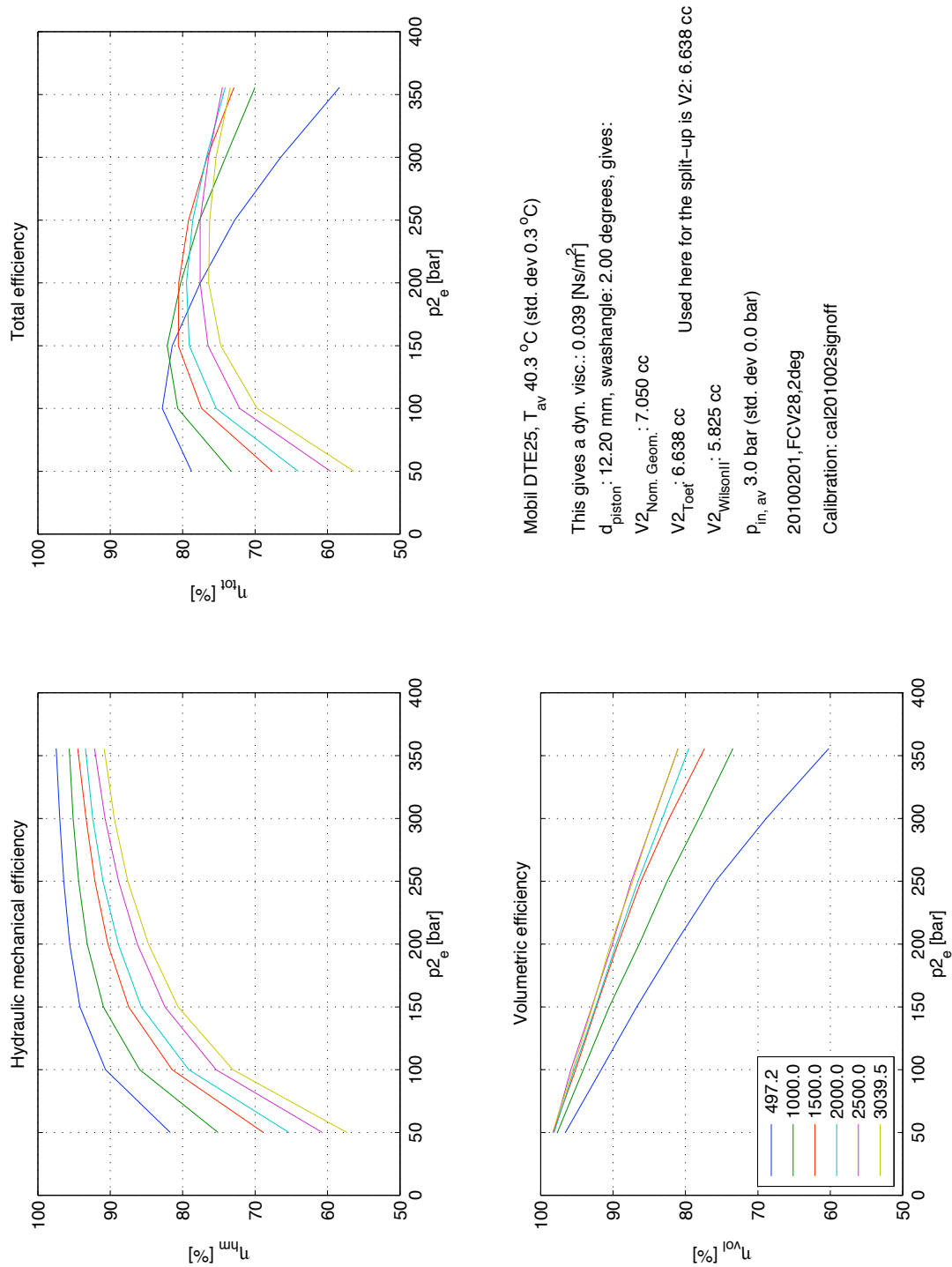


**Figure 19:** Efficiency curves, 2 degrees swash angle

## 8.5 Combination of errors (ISO 4409)

The systematic error in the calculation of the power or the calculation of the total efficiency of the pump can be calculated from the systematic errors of instruments (See annex B of standard ISO 4409).

The relative error in total efficiency of the pump due to error propagation can be defined as:

$$\frac{\delta \eta_t^P}{\eta_t^P} = \sqrt{\left(\frac{\delta q_v}{q_v}\right)^2 + \left(\frac{\delta p}{p}\right)^2 + \left(\frac{\delta n}{n}\right)^2 + \left(\frac{\delta T}{T}\right)^2} \quad (7)$$

In the setup of our test circuit mass measurement is applied for determining the volume flow rate. Accordingly relative errors due to mass- and time measurements and to the accuracy of density have to be used as a substitute of relative errors in volume flow measurements. Consequently from propagation of systematic error follows that:

$$\left(\frac{\delta q_v}{q_v}\right)^2 = \left(\frac{\delta m}{m}\right)^2 + \left(\frac{\delta T}{T}\right)^2 + \left(\frac{\delta \rho}{\rho}\right)^2 \quad (8)$$

The relative errors found in the calibration of the sensors (see appendix A.2) are used in equation (7) and (8) to calculate the relative error in total efficiency. Interpolation in relative errors of separate quantities is used to determine the data of relative error in total efficiency for the set of operating points of the pump. The results of the calculation of the relative error in total efficiency in case of full (100%) displacement of the pump are shown in figure 20.

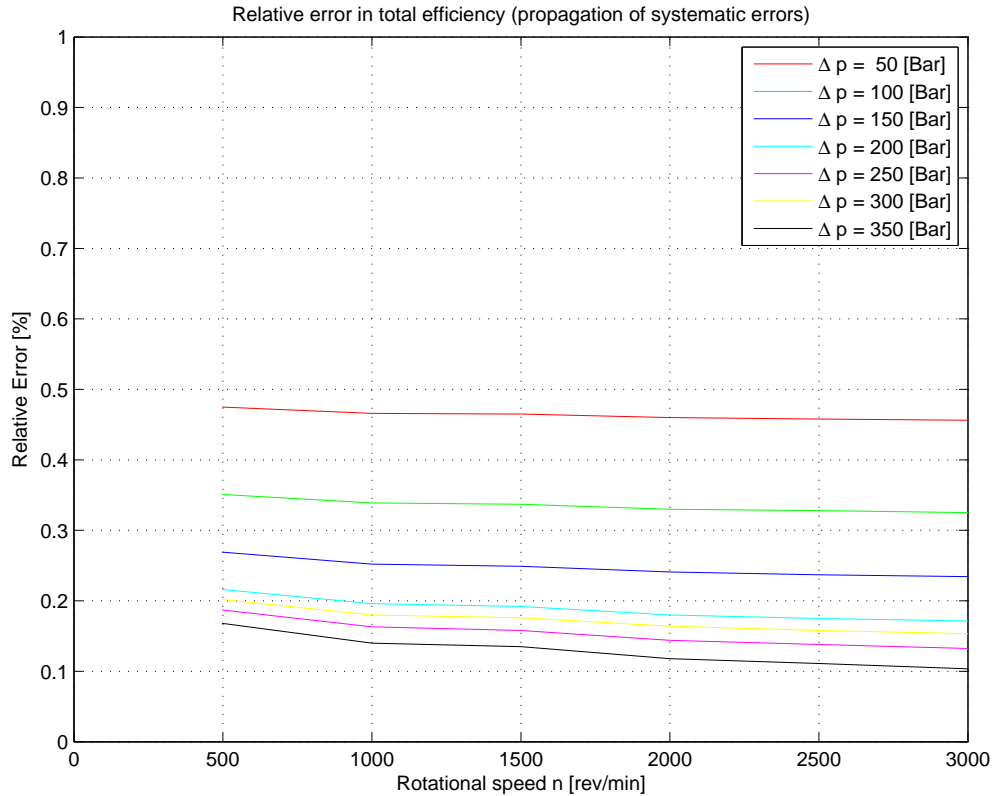


**Figure 20:** Systematic error in total efficiency at full (100%) displacement of the pump

Note that relative error is better than about 0.5% for the complete field of operating points and even better than 0.25% for most of the operating points. The lower end of the range of operating

points exhibits the worse values in accuracy.

Consequently the total efficiency determined for this pump at full displacement, closely following the standard of ISO 4409, are estimated accurate within a band of  $\pm 0.5\%$  in the lower end to  $\pm 0.25\%$  in the mid- and higher end of the range of operation points.

In case of a variable displacement pump both volume flow rate and torque will decrease with the decrease of the displacement of the pump. For that reason measurements of these quantities will be more at the lower end of the measuring range. Likely such measurements will be less accurate due to the increase of the relative error near the lower end of the measuring range (see the calibration of sensors in appendix A.2). So accuracy may deteriorate at lower settings of the displacement. However this is circumvented partly in our setup for determining the volume flow rate by using measurement of mass. By increasing the measuring time the mass of fluid will increase too, so this measurement can be performed in a more favorable part of the measuring range. This feature is one of the benefits of applying mass flow over volume flow measurements.

The measurements at the lowest set value of the displacement of the pump can be considered as the worst case for the accuracy.

The results of the calculation of the relative error in total efficiency in case of 25% of the displacement of the pump are shown in figure 21.

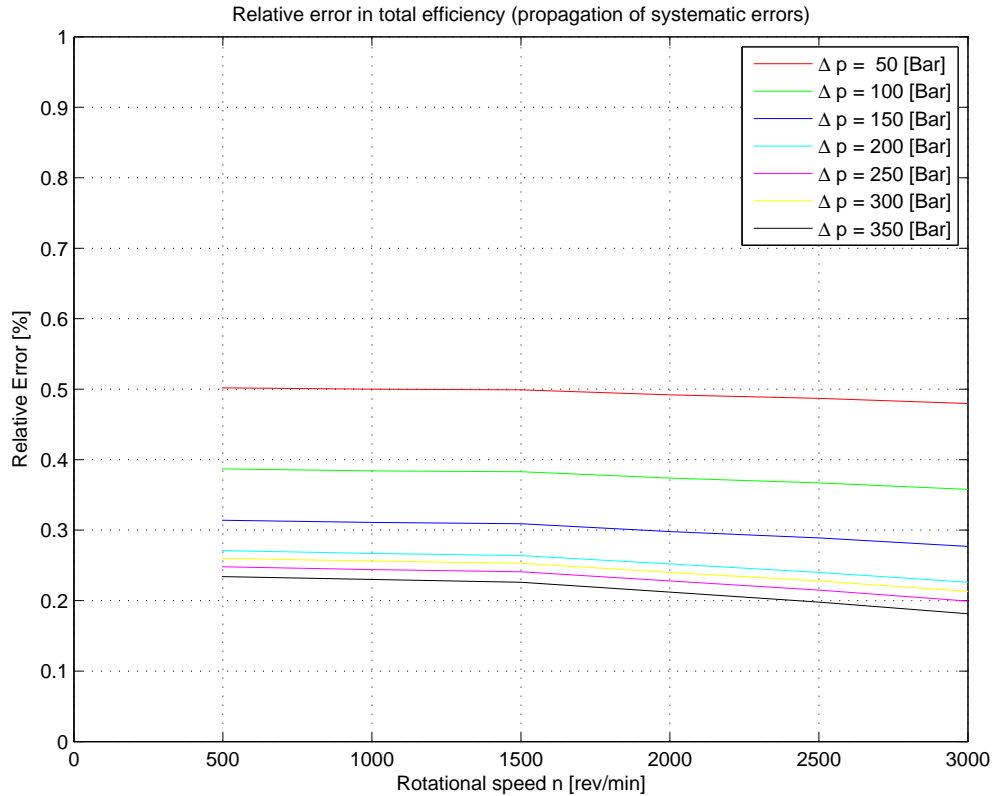


**Figure 21:** Systematic error in total efficiency at 25% displacement of the pump

Note that relative error is better than about 0.5% for the complete field of operating points, but no better than 0.25%. Generally it can be stated that the total efficiency determined for this pump at any displacement between 25% to 100%, closely following the standard of ISO 4409, are estimated accurate within a band of  $\pm 0.5\%$  to  $\pm 0.25\%$  or better near full displacement.

## 8.6 Conclusions of measurements

The total efficiency of the FCV28 type of variable pump in case of full displacement (i.e. 8 degrees swash angle) shows high values in a wide band of the operating points. At decreasing swash angles, the efficiencies also decrease, but only very gradually. This is in line with the expectations, as in the FC type of pump – due to the different kinematics of this concept – there are no pressure induced contact forces between the pistons and the cavities in which they run. With this, an important source of hydromechanical losses and stiction in the more conventional types of axial piston units, is avoided in the FC concept.

The derived capacities found for this pump (according to Toet [3]), for the four different swash angles measured, appear to be consistent with the measured data and the results for the part efficiencies (volumetric and hydro-mechanical). Applying these values in the calculation of the part efficiencies result in outcomes with a physical meaning, i.e. remain below or just up to the 100% mark for both of the part efficiencies. Physical meaning refers to the assumption that the pump is absolutely a positive displacement pump: the volume flow rate is generated exclusively by positive displacement.

It may be noted that measuring positive displacement pumps with such high performance stresses the methods for determination of performance according to the standard of ISO 4409 to the limits.

## References

- [1] Ivantysyn, J. and Ivantysynova, M. *Hydrostatic Pumps and Motors, Principles, Designs, Performance, Modelling, Analysis, Control and Testing*, Academia Books International, New Delhi, 2000.
- [2] Schlösser, W.M.J., Hilbrands, J.W. *Das theoretische Hubvolumen von Verdrängermaschinen*, Ölhydraulik und Pneumatik 7, Nr. 4, 1963.
- [3] Toet, G. *Die Bestimmung des theoretischen Verdrängervolumen von hydrostatischen Verdrängerpumpen und Motoren aus volumetrischen Messungen*, Ölhydraulik und Pneumatik 14, Nr. 5, 1970.
- [4] Wilson, W.E. *performance criteria for positive displacement pumps and fluid motors*, ASME semi-annual meeting, May-June 1948, paper nr. 48-SA-14.
- [5] Witt, K. *Die Berechnung physikalischer und thermodynamischer Kennwerte von Druckflüssigkeiten, sowie die Bestimmung des gesamtwirkungsgrades an Pumpen unter berücksichtigung der Thermodynamik für die Druckflüssigkeit*, Thesis Eindhoven University of Technology, Eindhoven, The Netherlands, 1974.
- [6] Witt, K. *Thermodynamisches Messen in der Ölhydraulik - Die Thermodynamik der Druckflüssigkeiten*, Ölhydraulik und Pneumatik 20 (1976) Nr. 9.



## A Appendix

### A.1 Classes of measurement accuracy ISO 4409 and ISO 8426

Tables 5, 6 and 7 according standard ISO 4409/ISO 8426 and table 8 according standard ISO 8426.

**Table 5:** *Permissible variation in indicated fluid temperature*

Class of measurement accuracy	A	B	C
Variation of temperature indication, K	$\pm 1.0$	$\pm 2.0$	$\pm 4.0$

**Table 6:** *Limits of permissible variation of mean indicated values of selected parameters*

Parameter	Permissible variation for classes of measurement accuracy		
	A	B	C
Rotational speed, %	$\pm 0.5$	$\pm 1.0$	$\pm 2.0$
Torque, %	$\pm 0.5$	$\pm 1.0$	$\pm 2.0$
Volume flow rate, %	$\pm 0.5$	$\pm 1.5$	$\pm 2.5$
Pressures, where $p < 2 \times 10^5$ Pa gauge, Pa	$\pm 1 \times 10^3$	$\pm 3 \times 10^3$	$\pm 5 \times 10^3$
Pressures, where $p > 2 \times 10^5$ Pa gauge, %	$\pm 0.5$	$\pm 1.5$	$\pm 2.5$

**Note:**

The permissible variations listed concerns deviation of the indicated instrument reading and do not refer to limits of error of instrument reading. These variations are used as an indicator of steady state, and are also used where graphical results are presented for a parameter of fixed value. The actual indicated value should be used in any subsequent calculation of power or efficiency.

**Table 7:** *Permissible systematic errors of measuring instruments as determined during calibration*

Parameter of measuring instrument	Permissible systematic errors for classes of measuring accuracy		
	A	B	C
Rotational speed, %	$\pm 0.5$	$\pm 1.0$	$\pm 2.0$
Torque, %	$\pm 0.5$	$\pm 1.0$	$\pm 2.0$
Volume flow rate, %	$\pm 0.5$	$\pm 1.5$	$\pm 2.5$
Pressures where $p < 2$ bar Pa gauge, bar	$\pm 0.01$	$\pm 0.03$	$\pm 0.05$
Pressures where $p > 2$ bar Pa gauge, %	$\pm 0.5$	$\pm 1.5$	$\pm 2.5$
Temperature, K	$\pm 0.5$	$\pm 1.0$	$\pm 2.0$

**Note:**

The percentage limits given in this table apply to the value of the quantity being measured and not to the maximum values of the test or the maximum reading of the instrument.

**Table 8:** *Pump and motor test speeds*

Classes of measurement accuracy	number of speeds	Speed movements over full continuous rated speed range
A	10 or more	In equal increments
B	5 or more	In equal increments
C	3 or more	At 20, 50 and 100%

## A.2 Errors and classes of measurement accuracy

Where appropriate, measurement devices (sensors and transducers) and measurement instruments (conditioning, amplifiers etc.) are calibrated in the measurement chain of the measurement set up. An exception is the calibration of the torque measuring shaft, which is calibrated together with its bridge amplifier on a separate test rig. A number of calibrations is based on the use of known and calibrated weights (NKO certified)). This is the case in the dead weight calibration apparatus (Barnet Instruments) for pressure devices, in the calibration of the weight system for the mass flow rate and in the test rig for calibration of torque devices. The pressure sensors, the torque measuring shaft and the bascule have been re-calibrated immediately after the measurements described in this report.

The rotational speed transducer has not been re-calibrated. This sensor has been introduced in this testbed in 2004, when its signal chain was also calibrated to an accuracy better than 0.1%. It has been in the testbed ever since. The signal quality of the optical disc sensor and the accuracy of the transformation to rotational speed, are checked on a very regular basis: using a scope which is always included in its signal chain, the raw pulses are monitored and the scope's frequency readout for this signal is compared with the speed reported by the LabView VI interface. The match is always in the range of that same 0.1%.

The drain flow sensor has been calibrated against the bascule for the last time in March 2007. The resulting linear fit was accurate to within 1% for very low flows. Above flows of 0.2 [Lpm], the accuracy was better than 0.5% improving to 0.1 % above 1 [Lpm]. In view of the very small impact of the accuracy of this flow measurement on the efficiency calculation, this sensor was not re-calibrated in the context of these measurements.

All calibrations, with the exception of the calibration of the differential pressure sensor, are based on linear regression (best linear line fit, least squares fitting) of the recorded data, resulting in data for the slope and the intercept of the fitted line. For the differential pressure sensor, a quadratic fit was used, in order to reach the required precision in the range of measurements. Each linear fit of the following calibrations shows a good relationship to a linear line. For the linear fits, the data for the slope and the intercept of the fitted lines have been used for the conversion to the physical quantities. For the quadratic fit of the pressure difference sensor, the 3 terms have been used that result from of a Matlab `polyfit` operation with a polynomial of degree 2. The graphical results of the most important calibrations are depicted in figures 22 to 25, together with the relevant data for the fits.

Also the error of the observed data to the linear fit is depicted as the relative error, defined by:

$$\begin{aligned} \text{relative error}[\%] &= \text{error} / \text{calculated value} * 100\% , \text{ where} \\ \text{error} &= \text{observed value} - \text{calculated value} \end{aligned}$$

Note that these graphs also show the boundaries of class A of the measurement accuracy (see also table 3 of appendix A.1).

## Calibration of the torque transducer

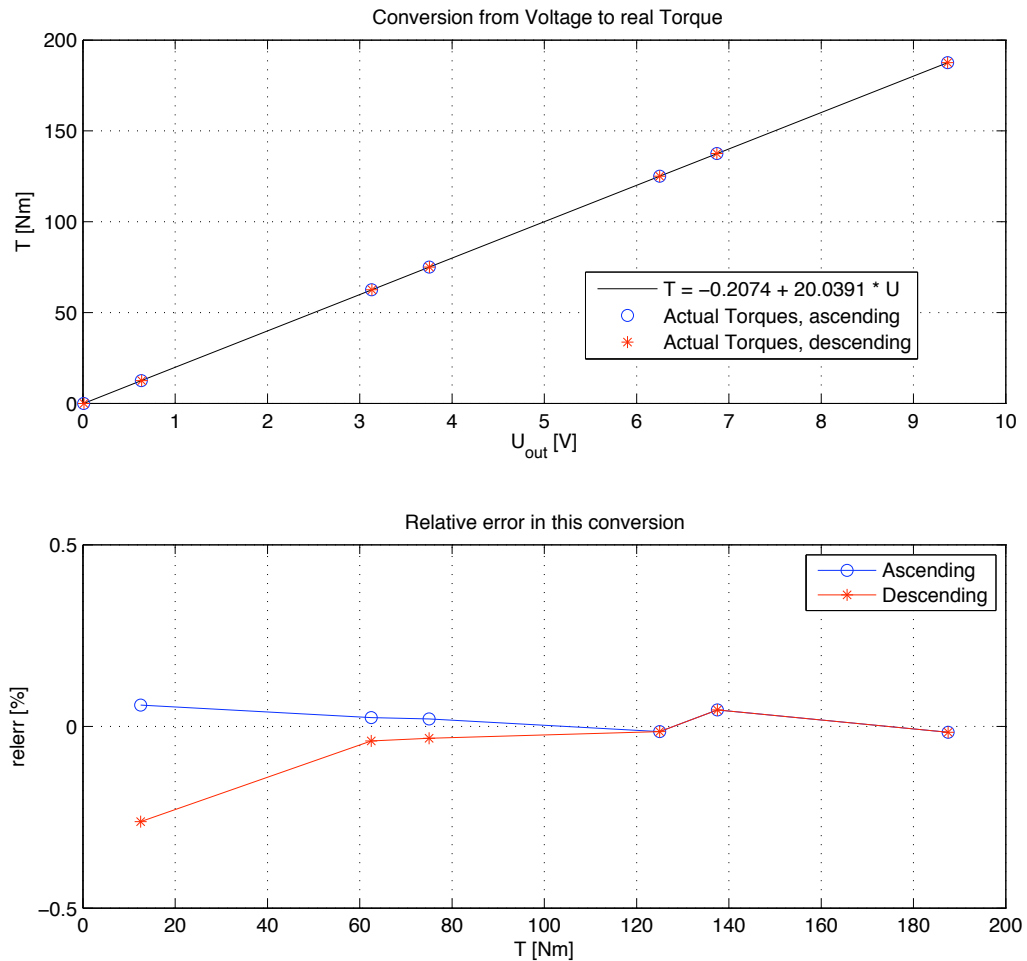


**Figure 22:** *HBM (Hottinger Baldwin Messtechnik) T2/200 Nm torque measuring shaft + HBM MGC strain-gage bridge amplifier (Calibration date: February, 4, 2010)*

## Calibration pressure transmitter inlet pump

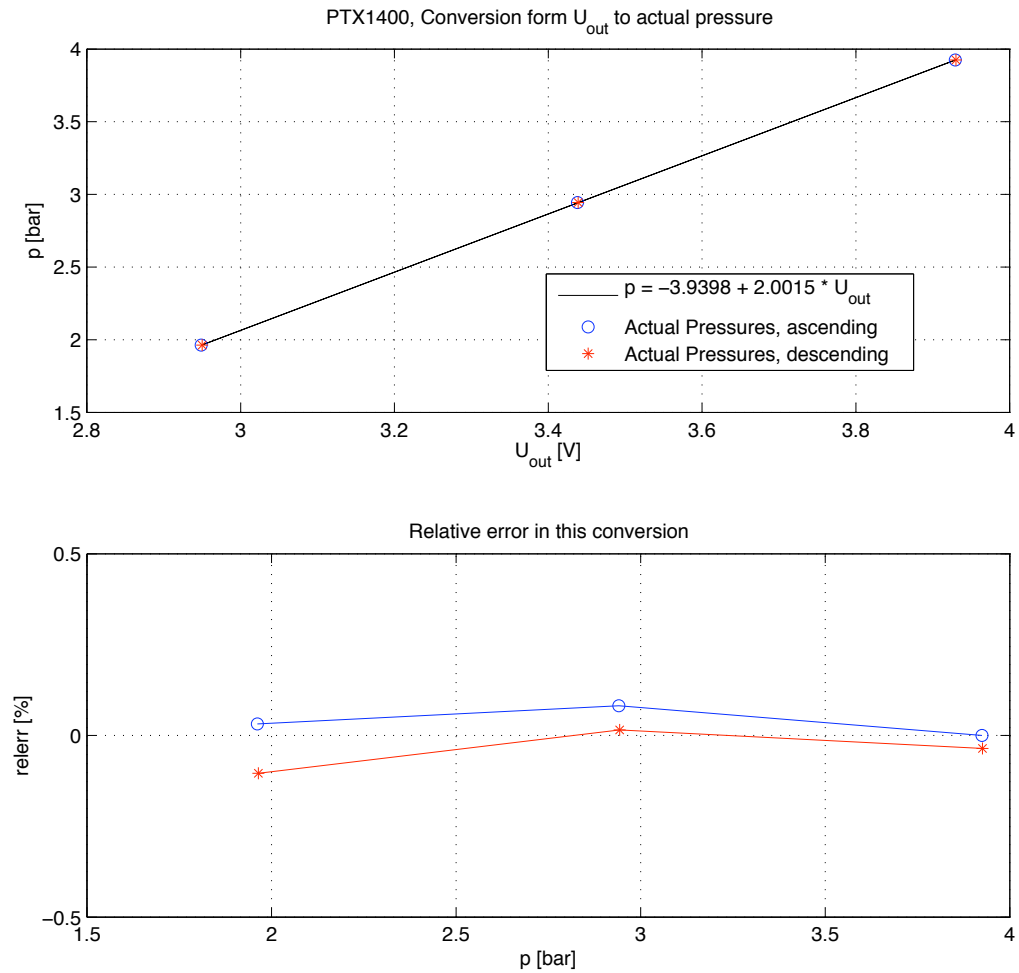


**Figure 23:** Druck PTX 1400 pressure transmitter 4-20 mA output  
(Calibration date: February, 1, 2010)

## Calibration pressure differential transducer

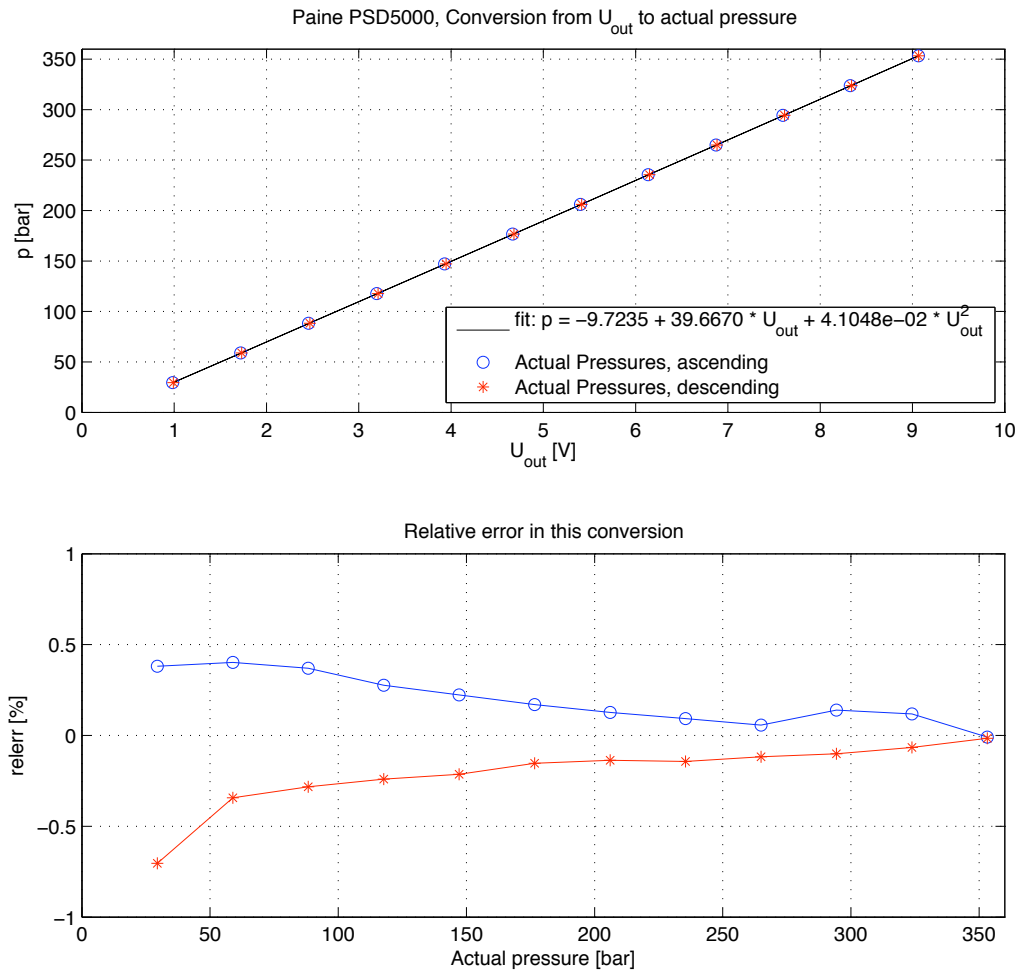


**Figure 24:** *Paine 5000 PSID Bi-directional differential pressure transducer + HBM MVD2555 strain-gage bridge amplifier (Calibration date: February, 1, 2010)*

## Calibration Bascule

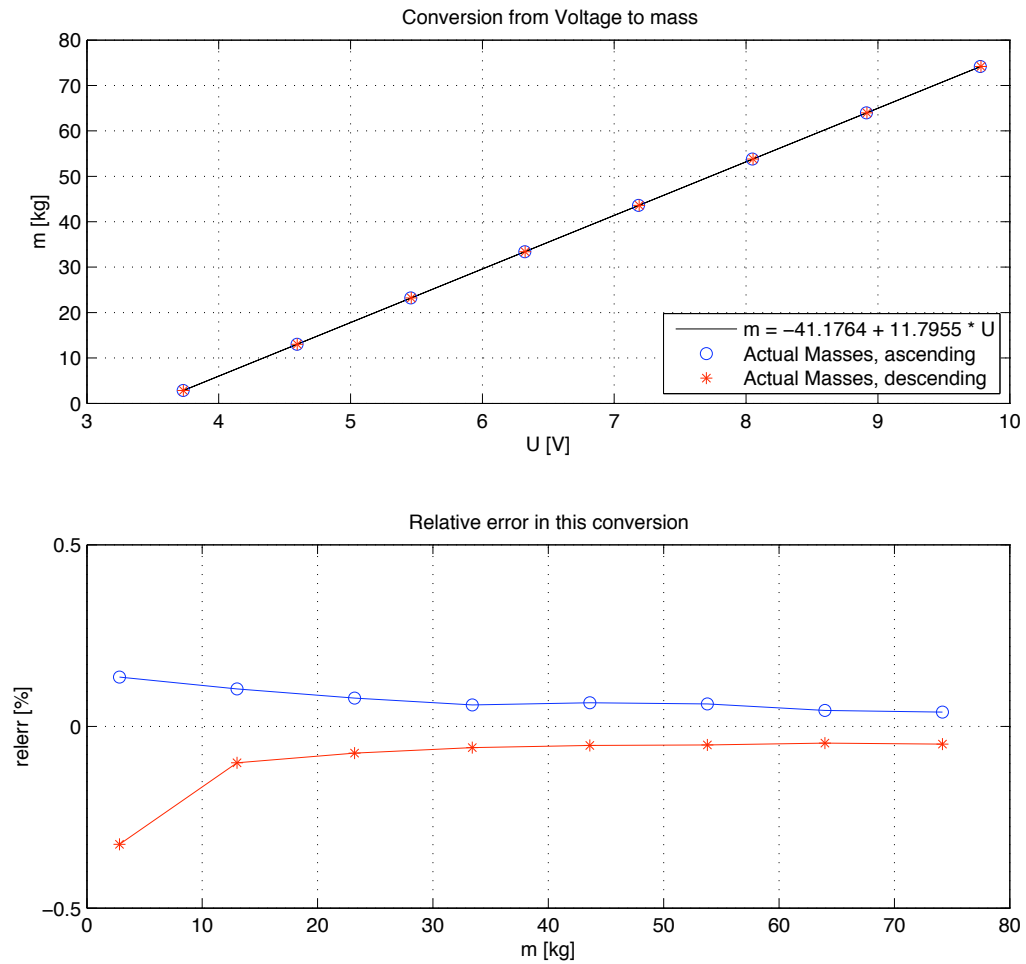


**Figure 25:** *Raute BA3 load cells (inclusive pendulum support mounting RGP10) + Logic DLC95-C Load cell indicator (Calibration date: February, 1, 2010)*